Transmit diversity methods for OFDM

Diplomarbeit

von

Frank Schühlein

Abteilung Telekommunikationstechnik und
angewandte Informationstheorie

Universität Ulm, April 2002

D/2001/AX/02

Ich versichere, dass ich die vorliegende Diplomarbeit selbständig und ohne unzulässige fremde Hilfe angefertigt habe.

Ulm, 17. April 2002

Frank Schühlein

Preface

This diploma thesis is the result of my work in the department of Telecommunications and Applied Information Theory at the University of Ulm.

First of all I thank Prof. Martin Bossert for his support and guidance. Further on I thank my tutors Axel Hübner and Bernd Baumgartner for their good and friendly attendance throughout this thesis and the fruitful discussions and cooperation. Beyond I want to thank all the post graduates and students in the department for the relaxed and pleasant ambiance.

Frank Schühlein, April 2002

Contents

1 Introduction

In the last years the field of communication technology crosses our mind more and more. Especially the high costs of the german UMTS license auction which results in approximately 50,8 billon Euro in total for the six participating companies respective investor groups arrested attention. Besides the number of used cellular phones has risen dramatically during the last years which points up the relevance of mobile communication nowadays. But not only the speech transmission has evoked an enormous demand in this area. Especially the increasing need of wireless local data networks (WLAN) for computers, personal digital assistants (PDA) and peripheral devices is responsible for high research activities. But also broadcasting services as e.g. digital radio and television require advanced transmission techniques for mobile applications at different velocities. First mentioned has already started in Germany (2000) and the second mentioned will start in summer 2003. Until 2010 television broadcasting should completely be digitalised.

Future requirements to the service quality and usability will continue to rise and can be characterised by permanent availability, mobility, high and reliable data rates. In addition the mobile devices have to be small and grant a long utilisation time concerning the battery live-time. These demands result from the high expenses of researches and bandwidth licenses. Comprising can be said that we need improved methods to master these demands.

In this thesis we want to investigate Orthogonal Frequency Division Multiplexing (OFDM) in combination with spatial diversity which denotes the use of multiple antennas. First mentioned is well suited to cope with the problems of mobile radio channels as e.g. the multi-path propagation. Due to the increasing data rates more bandwidth is required which has to be exhausted efficiently. Therefore we have to prevent time and computation intensive decoding methods as e.g. the equalisation process. They are also responsible for the power consumption and the costs for the required processor performance. OFDM provides an effective scheme to fight these problems by using a simple equalisation method and a guard time to circumvent Inter-Symbol-Interferences.

The second item mentioned above is the demand for high reliability and a low bit error rate. By using multiple antennas we want to exploit the space dimension to improve the transmission performance without using additional bandwidth. In this thesis we only want to consider transmit diversity because we assume the downlink scenario of a fixed base station. This can be extended with more transmitter relatively simple. Whereas the small mobile device struggles with the problems of size, power supply and low costs. Due to these requirements it is difficult to integrate multiple receive antennas, expensive and energy consuming decoding devices. Further we can increase the fault tolerance of the transmission system

because of the multiple antennas which may keep the connections alive even if one antenna fails.

OFDM, which is the basis for the following transmission schemes is briefly described in section 2 and some characteristics are investigated.

Section 3 deals with spatial antenna diversity with special consideration of Cyclic Delay Diversity (CDD). We explain the three implementation possibilities and describe the influence on the transmission characteristics. Besides it is compared with the performance of an interleaver.

In section 4 we have a look at the Alamouti scheme and its combination with OFDM. We obtain two implementation possibilities and propose a new decoding method to cope with the problems on time and frequency variant channels. Further on techniques to decode to hard decided bits respective soft values are presented.

In section 5 we finally consider a combination of a variant of the Alamouti scheme and CDD. First it is described and investigated and then it is extended to more antennas.

Section 6 finally concludes this work and summarises the main results.

2 Fundamentals of OFDM

In this section we present *Orthogonal Frequency Division Multiplexing* (OFDM). The principles of multi-carrier transmission are already known since the late sixties [16] [4]. The bandwidth is thereby subdivided into a set of subcarriers. In OFDM the subchannels have to be orthogonal. This orthogonality criterion does not mean that the subbands must not overlap. Further they can be viewed as low rate subchannels with small bandwidth, where the sent signal is the sum of multiple symbols being transmitted in parallel. Therefore the channel fractions can be viewed as flat-fading channels for a suited small subcarrier bandwidth. Besides we can therewith overcome the problem of narrow-band distortion because the appropriate carriers stay simply unused or a water-filling method is applied. Also the equalisation can be simplified due to the flat-fading case. Further this scheme has an effective method to cope with Inter-Symbol-Interference (ISI) resulting from multi-path propagation of mobile channels which is often very difficult to solve. Especially the complexity and the therewith connected temporal duration and hardware efforts play an important role.

Although multi-carrier modulation and OFDM are already known for several years, the hardware expense was high and this was therefore a reason against an implementation. The traditional direct form of realisation is especially for high numbers of subcarriers complex. Each subcarrier is thereby implemented with its own signal path (increase of the sampling rate, filtering, complex multiplication for the frequency shift and summation of all subsignals). But with improved signal processing technology it becomes more and more interesting. Another possibility was presented by Weinstein and Ebert [21] using the Discrete Fourier Transform (DFT) and the Inverse DFT (IDFT). This simplifies the description and realisation because now low priced chips performing this task are available.

OFDM is already or will be used in the following transmission systems [2]:

- European terrestrial digital television, Digital Video Broadcasting (DVB-T), Digital Terrestrial Television Broadcasting (DTTB) and High Definition Television (HDTV)
- Digital Audio Broadcasting (DAB) (developed by the EU research initiative EUREKA 147, uses Coded OFDM)
- Powerline
- HIPERLAN/2 (according to IEEE 802.11a standard) with up to 54 Mbit/s

- Some Digital Subscriber Lines (DSL) technologies, like High-bit-rate DSL (HDSL, up to 1.6 Mbit/s), Asymmetric DSL (ADSL, up to 6 Mbit/s) and Very-high-speed DSL (VDSL, up to 100 Mbit/s)

In the following a short overview over OFDM and related topics is given. A more detailed description can be found in [6].

2.1 Transmission model

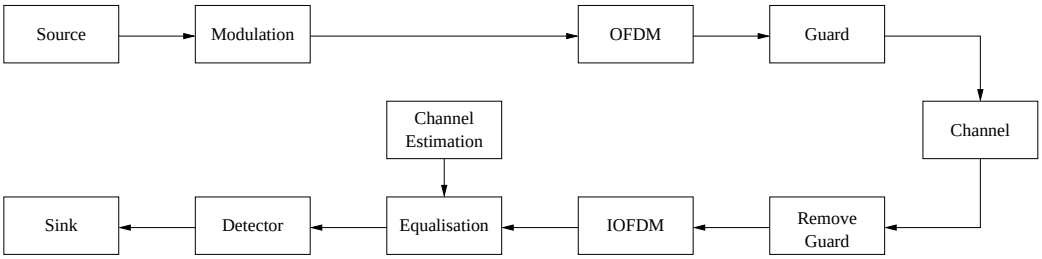

Figure 1: OFDM transmission model

In figure 1 the basic OFDM transmission model used in this work is depicted. Only in the equalisation part we have some exceptions later on.

We assume a source supplying a binary data stream. These bits are mapped to complex symbols using a modulation alphabet A_x. The modulator encodes $m = \log_2 M$ with $M = |A_x|$ bits to one symbol. In this work we use BPSK modulation $A_x = \{0 \to 1,\ 1 \to -1\}$. Afterwards the OFDM modulation is performed which is described in more detail in subsection 2.2. In this module a serial to parallel multiplexing is followed by a block by block Inverse Discrete Fourier Transform which assigns the complex results to the N_F subcarriers.

To avoid Inter-Symbol-Interferences caused by multi-path propagation we add a guard time of N_G with $N_G \leq N_F$ time slots in front of each block. It has to be longer than the maximum delay of the channel so that the preceding symbol is completely decayed when the next symbol starts. This guard time is created with the last N_G elements (cyclic extension) of the OFDM symbol. This is important to keep orthogonality. It can get lost due to initial oscillation effects during a hard change-over from guard time to OFDM symbol [14]. Despite it is useful to keep synchronisation which would be more difficult compared to an empty time period [22]. On the other hand a long guard time leads to a rate and SNR loss. Therefore we try to keep it as short as possible. The SNR loss in dB and the decrease of the rate can be calculated as follows [6]:

$$\Delta SNR = 10\log_{10}\frac{N_F + N_G}{N_F} \qquad \Delta R = \left(1 - \frac{N_F}{N_F + N_G}\right) \cdot R_0. \tag{1}$$

Here ends the considered part on the transmitter side. The following steps of the transmission, e.g., D/A conversion, output filters, bandpass representation, HF part, ..., are not concerned. The channel is described in subsection 2.3.

On the receiver side we start our investigations on the same level as we ended before. Therefore the first step is to remove the guard time from the symbol stream because it only contains the parts of the multi-path propagation of the preceding symbol. Afterwards the OFDM encoding is reversed using the block by block Discrete Fourier Transform which is also described in subsection 2.2. From the resulting output a channel estimation is extracted which can e.g. be done with pilot information within the whole OFDM symbol. The estimation is used to reverse the influence of the channel. This process is called equalisation. The topic is closer investigated in subsection 2.3. The resulting symbols are then fed to the detector which decides to bits respective delivers soft values according to the modulation alphabet. For the first mentioned it reverses the symbol mapping into a binary bit stream. For later channel coding within the data sink it is often desirable to use the second option because we can reach additional gains using these reliability informations during the decoding process.

2.2 Realisation of multi-carrier modulation

In this subsection we want to look at the OFDM modulation itself. There are two equivalent approaches. The first option is called the direct realisation using the block diagram in figure 4. The second version is to describe it with the Inverse Discrete Fourier Transform (IDFT) on the sender side respective the Discrete Fourier Transform (DFT) in the receiver.

First we want to have a look at the first form which is well suited to give a glance of what is done in OFDM modulation. The following description should only be a short overview. For further explanation we refer to [6].

In figure 2 our goal is displayed. We subdivide the bandwidth in N_F narrow subbands. We assume the channels to be constant in each of the subchannels. Therefore we approximate them as flat-fading channels. The advantage here is that we have only one complex channel value for each carrier. This simplifies our equalisation process. There we try to reverse the influence of the channel. But we will deal with this topic later.

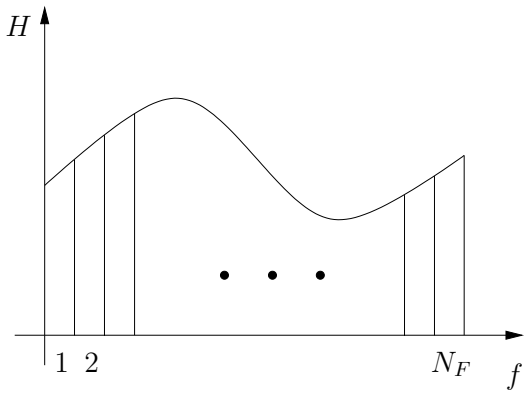

Figure 2: Fragmentation of the bandwidth into subbands

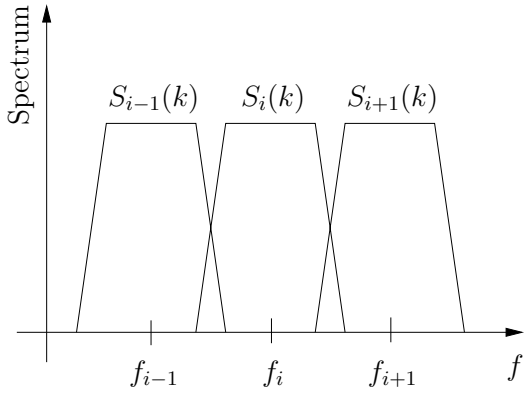

Figure 3: Spectrum of the subcarriers

The modulation scheme is illustrated in figure 3. The spectrum of a chosen filter with transfer function $g(l)$ is shifted to frequency f_i and weighted with the complex transmit symbol $S_i(k)$.

In figure 4 the block diagram of the direct realisation of the modulation scheme as mentioned above is depicted. The complex sequence $\mathbf{S}$ with sampling rate $1/T_{s,0}$ is divided into blocks with N_F symbols $S_0(k), \ldots, S_{N_F-1}(k)$. This process is called demultiplexing or serial-to-parallel conversion. To perform the later impulse shaping with the filter $g(l)$ we have to upsample by $M = T_{s,0}/T_s$ and obtain a new sampling rate $1/T_s$ with time index l

$$S_i^{up}(l) = \begin{cases} S_i(k) & \text{for } l = kM \\ 0 & \text{for } l \neq kM \end{cases}, \quad i = 1, \ldots, N_F. \tag{2}$$

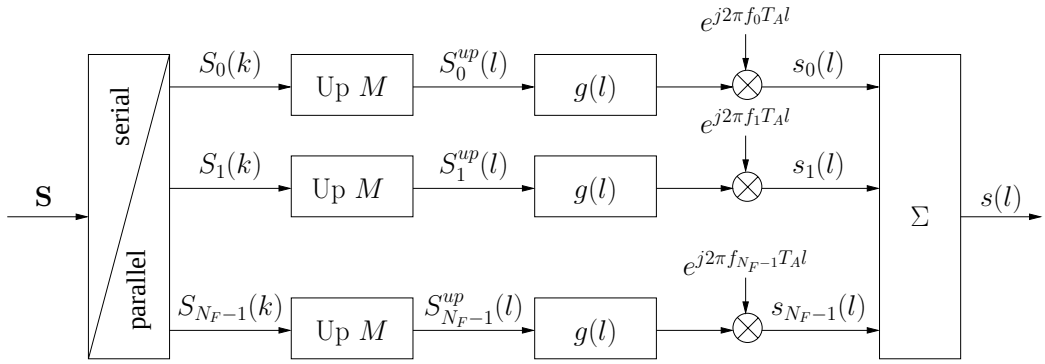

Figure 4: Block diagram of the direct realisation

Afterwards the filtered signal is shifted to the appropriate frequency f_i. Normally we subdivide the bandwidth $W = 1/T_s$ in equally spaced subbands. Therefore we can write $f_i = i \cdot \Delta f$ with $\Delta f = W/N_F$. The resulting subsignals $s_i(l)$ can then be written as

$$s_i(l) = \left(S_i^{up}(l) * g(l)\right) \cdot e^{j2\pi f_i l T_A} = e^{j2\pi f_i l T_A} \cdot \sum_{\nu=-\infty}^{\infty} g(\nu) S_i^{up}(l-\nu) \tag{3}$$

where $*$ denotes the convolution operator. We obtain for the overall signal

$$s(l) = \sum_{i=0}^{N_F-1} s_i(l) = \sum_{i=0}^{N_F-1} e^{j2\pi f_i l T_A} \cdot \sum_{\nu=-\infty}^{\infty} g(\nu) S_i^{up}(l-\nu). \tag{4}$$

By using different choices of the filter $g(l)$ the spectral characteristics can be influenced [6]. But for us only the rectangular filter $g(l) = 1$ for $l = 0, \ldots, N_F - 1$ is interesting. There we can simply omit it and furthermore we keep orthogonality between the subcarriers.

This leads us directly to the other description of the OFDM modulation using the Discrete Fourier Transform and its inverse. The transmission scheme can be described based on the following equations [21]:

$$\begin{aligned} \text{IDFT}_N: \quad x_n &= \frac{1}{N} \sum_{k=0}^{N-1} X_k \cdot e^{j\frac{2\pi}{N}kn} \\ \text{DFT}_N: \quad X_k &= \sum_{n=0}^{N-1} x_n \cdot e^{-j\frac{2\pi}{N}kn}. \end{aligned} \tag{5}$$

Now we can easily calculate the OFDM modulation. We obtain the transmit values $s_i(k)$ by employing the IDFT on the symbols $S_i(k)$ with $i = 0, \ldots, N_F - 1$ of the N_F subchannels:

$$(s_0(k),\, s_1(k), \ldots, s_{N_F-1}(k)) = \mathrm{IDFT}_{N_F} \{(S_0(k),\, S_1(k), \ldots, S_{N_F-1}(k))\}\,. \qquad (6)$$

Analogously we get for the Inverse OFDM:

$$(S_0(k),\, S_1(k), \ldots, S_{N_F-1}(k)) = \mathrm{DFT}_{N_F} \{(s_0(k),\, s_1(k), \ldots, s_{N_F-1}(k))\}\,. \qquad (7)$$

Here we do not want to go deeper into the theory of OFDM. In [6] and [19] a detailed investigation on this topic can be found.

2.3 The channel model and OFDM

In this subsection we want to have a look at the transmission media in special consideration of the interaction with OFDM. In this thesis we only want to concentrate on mobile radio channels. First we introduce the channel model and its characteristics and then we have a look at its combination with OFDM.

The channel behaviour is strongly influenced by the carrier frequency f_c and the bandwidth W of the transmission. Besides we suppose that we have a fixed and higher situated base station. The mobile receiver is surrounded by nearby scatterer. This leads to multi-path spread, which means that the signal is received from several different paths with different strengths. Therefore time shifts occur which leads to Inter-Symbol-Interference (ISI). The maximum delay is identified with τ_m. The current symbol can then be superimposed by previous ones. Because the mobile user moves and/or the surrounding scatterer change we face a time-variant environment. These effects cause time-dependent fading. This means that certain or even all frequencies are attenuated respective erased. Besides we get an effect called Doppler shift. It is a measure for the speed of the channel variation. The parameter $f_{D,\,max}$ is called the maximum Doppler shift that appears and can be calculated as follows:

$$f_{D,\,max} = \frac{v \cdot f_c}{c}, \qquad (8)$$

where v denotes the velocity of the mobile receiver and c the speed of light. We can now give two measures for the channel variance. The first is the coherence bandwidth $\Delta f_c \approx 1/\tau_m$. The second is the coherence time $\Delta T_c \approx 1/f_{D,\,max}$ [13]. Summarised is all this under the term Wide Sense Stationary Uncorrelated Scattering (WSSUS) channel model which is used in this work.

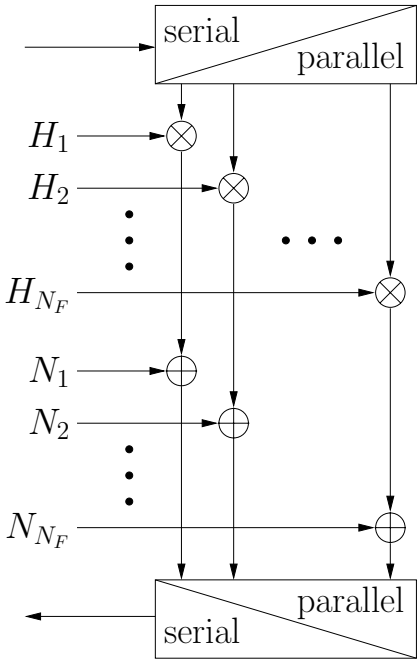

Figure 5: Channel model of a parallel transmission over flat-fading channels

OFDM provides N_F parallel subchannels which are orthogonal to each other. This is achieved by using N_F subcarriers with different frequencies f_i with $i = 0, \ldots, N_F - 1$, and bandwidth $\Delta f = W/N_F$. They subdivide the total bandwidth W. We make the approximation that these subchannels are narrow and they can be regarded as flat-fading channels. Each of them consists of a multiplication with a complex channel coefficient $H_i = \alpha_i \cdot e^{j\theta_i}$ and an additive, complex noise component N_i which is uncorrelated to the others. In figure 5 the channel model is depicted. Each transmitted symbol is therefore rotated by θ_i, weighted by α_i, and shifted in the complex plane by N_i.

This leads directly to the reason why the approximation of narrow subchannels is very useful. To get optimal decoding performance we try to reverse the channel influence. This process is called equalisation. Of course we need a channel estimation for this purpose. This can be done using pilot channels or sequences, respectively. Known subcarriers respective time slots are reserved for the estimation. This reduces the data rate and we have to weigh between exactness and rate loss. Due to the channel model described above, the equalisation simplifies to a multiplication with the inverse of the appropriate channel value H_i. This is much easier compared to other transmission schemes. The estimated sent symbol $S_{i,\,eq}$ is therefore:

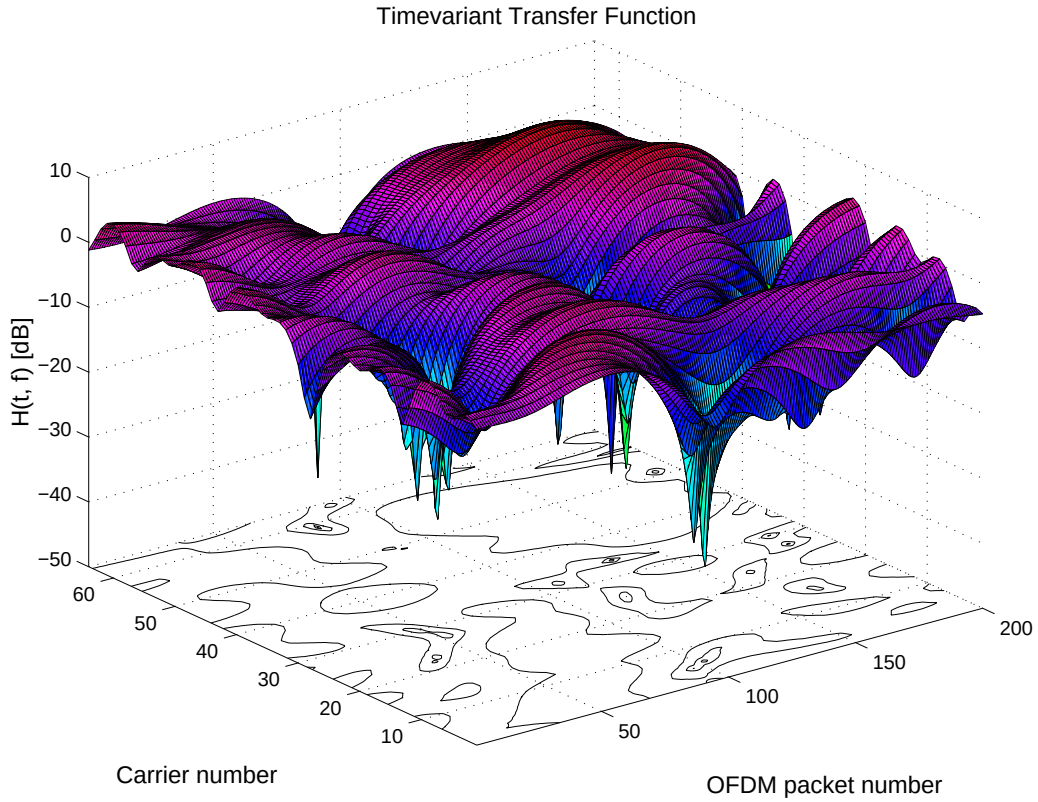

Figure 6: Six path channel with $\tau_m = 0.5\mu s$, $v = 500$ km/h, $W = 20$ MHz

$$S_{i,\,eq} = \frac{1}{H_i} \cdot R_i = \frac{1}{H_i}\left(H_i \cdot S_i + N_i\right) = S_i + \frac{N_i}{H_i}, \qquad i = 1, \ldots, N_F \tag{9}$$

where R_i denotes the received and S_i the sent symbol. This approach is called Zero-Forcing (ZF) equalisation [13]. The additive noise is thereby ignored because it cannot be estimated. Only statistic parameters can be determined with additional effort. The simplicity of the technique has its problems, too. In equation (9) we notice that the noise component is neglected in the equalisation calculation. Therefore it is not reversed. Further on channels with strong attenuated subchannels $|H_i| = \alpha_i \approx 0$ cause the noise level to be increased strongly at the specific position (Noise Enhancement). This effect can be minimised using the Minimum Mean Square Errors (MMSE) approach which merges into ZF for increasing SNRs [15]. But there we have to perform a variance estimation of the noise which leads to an additional effort. Here we only use the ZF method to cope with the channel rotation and attenuation.

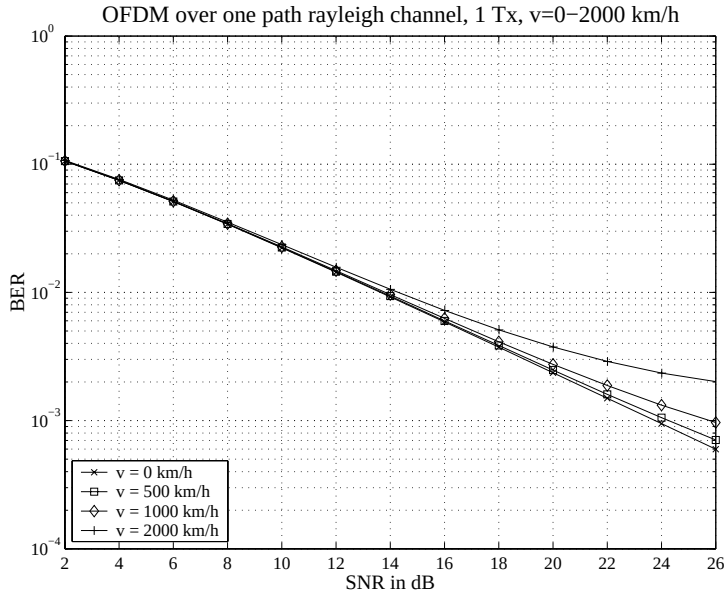

Figure 7: Uncoded OFDM transmission over a one-path Rayleigh fading channel with different velocities

In figure 6 an exemplary time-variant channel transfer function is displayed to show the problem we face. As channel model a six path channel with sampling time $T_s = 50$ ns, maximal channel delay $\tau_m = 10 \cdot T_s = 500$ ns, and maximal Doppler frequency $f_{D,\,max} = 2.38$ kHz without AWGN is used. We notice that the channel varies in frequency and time dimension.

Using the OFDM transmission scheme from figure 1 plus sufficiently complex channel coding we can give the channel capacity (normalised to the bandwidth) for each subcarrier *i* depending on the current channel state [6]:

$$C_i(E_i,\, H_i) = \log_2\left(1 + \frac{|H_i|^2 E_i}{N_0}\right), \tag{10}$$

where E_i is the energy of the *i*-th subcarrier and H_i is the corresponding channel value. $N_0/2$ denotes the spectral noise density.

Finally we look at the result of the previous considerations. In figure 7 the BERs of uncoded OFDM transmissions are displayed. The velocities are chosen from a wide range to point out their influence. Despite their impact depends highly on the used bandwidth. With an increasing speed OFDM performs worse. This is caused by the unmatched channel estimation and the Doppler shift. At the beginning of each OFDM symbol we determine the current channel state used to

calculate the equalisation values. For high velocities we face the problem that the channel changes within the OFDM symbol. This leads to a loss of the subchannel orthogonality and Inter-Channel-Interference (ICI). Only for $v = 0$ km/h we possess a perfect channel estimation because then we have a time-invariant channel. In subsection 4.4 we face this problem with Alamouti which is higher ranked in the transmission chain.

2.4 Properties of OFDM and related topics

OFDM becomes more and more popular due to its well-suited features e.g. for mobile radio channels. Therefore we want to describe its different characteristics. Despite we do not want to be restricted only on OFDM itself but we have a look at the whole transmission, too. In the following a brief overview is given:

- OFDM transforms the channel into N_F Rayleigh fading subchannels. Each of them can therefore be described as $R_i = H_i \cdot S_i + N_i$, with $i = 1, \ldots, N_F$, where S_i is the sent symbol, H_i is the complex channel value and N_i is the appropriate complex noise. We finally receive R_i.

- Due to the upper characteristic we can simplify the equalisation process to a Zero-Forcing (ZF) approach with low complexity. It tries to reverse the influence of the channel by dividing with the appropriate impulse response value. The negative aspect is the therewith coherent noise enhancement. Additionally we have the possibility to include the noise by using the Minimum Mean Square Errors (MMSE) algorithm. Apart from the needed channel estimation we have then to estimate the noise variance. Both versions are simple to implement and they are not too challenging for modern signal processing concerning computation complexity and memory.

- An OFDM transmission shows robustness against narrow-band distortion and it can easily be adapted to the current channel. First this can be done concerning the energy per carrier. There we have different choices like the water-filling principle to optimise the energy distribution on the carriers. A second possibility is that we can exclude certain frequencies which show a high noise level or narrow-band fading. On the other hand we can use the better subchannels to transmit with a higher data rate. This can be done e.g. using a modulation alphabet of higher order. Restricting we have to mention the necessity of a channel estimation on the transmitter side. Therefore we need a reverse channel which may cause problems due to the delay. This becomes important especially for fast time variant channels when the returned estimation can not be regarded as valid anymore.

- The essential guard time is well suited to cope with multi-path propagation as long as $\tau_m < N_G \cdot T_s$. It prevents following OFDM symbols from Inter-Symbol-Interferences (ISI). The problem is the choice of the guard length. If it is too long we face a high rate and SNR loss and otherwise we have ISI.

- A problem of OFDM is its high sensitivity against synchronisation errors [12]. Due to the narrow-band subchannels it is more prone to errors considering the carrier frequency and the subcarrier/-band division compared to single carrier systems. A mismatch in the first mentioned leads to a shift of the spectrum. The second error type is caused by differing sampling rates and this results in subchannel crosstalk. Further we have to deal with the problem of symbol synchronisation which is necessary for correct demodulation [6].

- Another problem is the high Peak-to-Average ratio. The OFDM signal has sometimes very high signal peaks resulting from certain symbol constellations. This requires a high linearity of the amplifiers (expensive) to prevent the transmission from Inter-Channel-Interference (ICI). Further it has to be driven far below the maximal amplification (inefficient). Otherwise we have to use algorithms which prevent these peaks by avoiding the critical symbol patterns. But on the other hand this reduces the usable rate [6].

- One assumption of OFDM is the subchannel orthogonality. It can get lost due to a fast changing channel. This causes ICI.

- In this thesis we assume a hard switch-over at the symbol borders. Therefore high out-of-band power might occur which disturbs neighbouring frequencies. We have two choices to fight this problem: The first option is to use additional filters to limit the spectrum. The second possibility is to include the filtering process in the modulation scheme by using suited filter functions $g(l)$ in figure 4 which are different to the rectangular.

3 Spatial antenna diversity

In this section we want to deal with spatial antenna diversity and OFDM. Therefore we study *Delay Diversity (DD)*, *Cyclic Delay Diversity (CDD)* and *Phase Diversity (PD)* that were introduced in [5]. These techniques can easily extend existing OFDM systems. In particular we investigate the effects of this diversity by the example of CDD. Therefore we first have a look at the uncoded transmission and the corresponding transformation of the channel. Afterwards we extend the system with channel coding and observe its effects. As spatial antenna diversity lowers the error density we compare it with an interleaver which tries to spread the errors of e.g. a flat-fade over a long period so that the convolutional decoder can correct them. Finally we investigate the result of a combination of the two mentioned methods and then draw the conclusions.

3.1 Introduction to spatial antenna diversity

3.1.1 Delay Diversity (DD)

One possibility to introduce the above mentioned diversity is to delay the signals on one or more different antennas. This was first described in [11]. Figure 8 shows an OFDM system as block diagram with N transmit antennas and DD. The OFDM modulated signal is extended by a guard interval with length $T_{guard} = N_G \cdot T_s$ and then it is transmitted over N antennas. The particular signals only differ in an antenna specific delay δ_n with $n = 1, \ldots, N-1$. This transmission is represented by the different uncorrelated channels $CH_0, \ldots, CH_{N-1}$. The signals superimpose in the receive antenna. On the receiver side the guard interval is removed and the Inverse OFDM (IOFDM) is performed. Because of the linearity, it is also possible to implement the time shifts on the receiver side. This can be treated analogously but then we have to deal with multiple receive antennas. Here we only want to investigate multiple transmit antennas and one receive antenna.

To avoid Inter-Symbol-Interference (ISI) it is obvious that the system has to fulfil the following condition:

$$\delta_n \leq T_{guard} - \tau_m, \quad n = 1, \ldots, N-1 \qquad \text{with} \quad T_{guard} \geq \tau_m, \tag{11}$$

where τ_m denotes the maximal multi-path delay spread. Because we want to maximise the usable transmission time we have to minimise the guard time T_{guard} to be only slightly larger than τ_m. Therefore the choice of δ_n is strongly restricted.

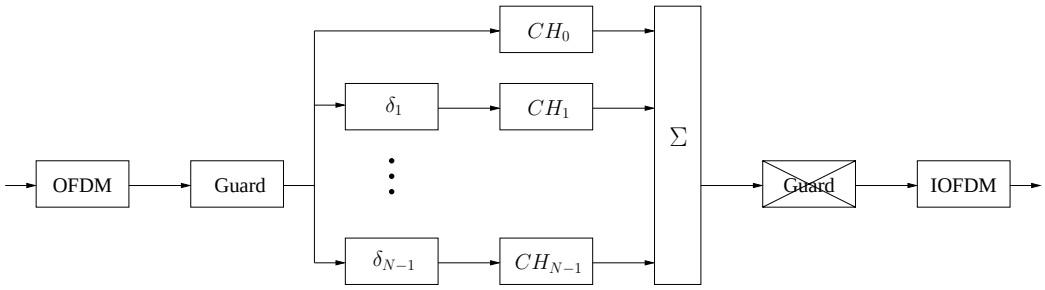

Figure 8: Delay Diversity on transmitter side

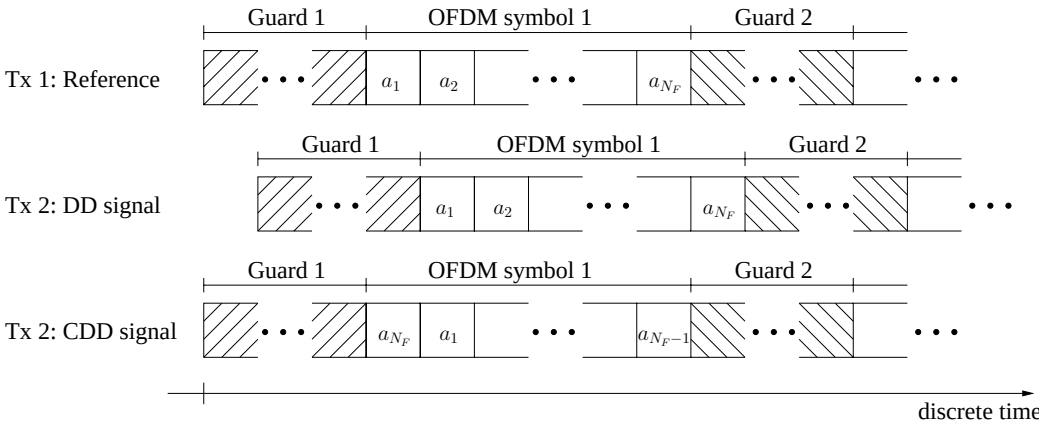

Figure 9: Difference between DD and CDD

3.1.2 Cyclical Delay Diversity (CDD)

CDD as described in [5] solves two main disadvantages of DD. One is the restriction to the choice of the delays δ_n. The other one is that an OFDM symbol partly overlaps with the guard interval of the following. Figure 9 shows the transmission of two consecutive OFDM symbols and therewith illustrates the differences between DD and CDD in time domain: The signal on the second antenna Tx 2 is delayed by one for DD and cyclically shifted for CDD respectively. In the figure a_i, with $i = 1,\ldots,N_F$, represents an OFDM modulated sample of the first symbol in the time domain. Here only time shifts which are multiples of the sampling time are shown. Otherwise some kind of time domain interpolation has to be done, which increases the complexity.

In figure 10 the block diagram for CDD is depicted. After the OFDM modulation the signal is split up to the different antennas and is then cyclically shifted with a specific delay δ_{cyn}. A prefix is added to fill the guard time. In difference to DD

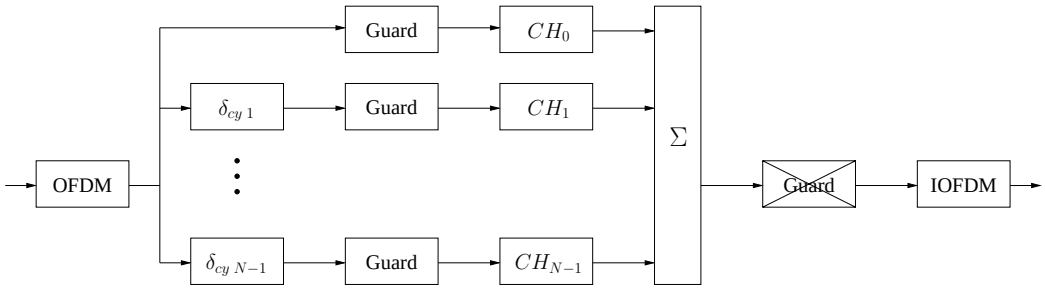

Figure 10: Cyclical Delay Diversity on transmitter side

cyclic shifts are used instead of time delays. Therefore it is necessary to implement the prefix as guard time after the cyclic time shift.

3.1.3 Phase Diversity

Phase Diversity is the equivalent representation of CDD in the frequency domain. Therefore it has to be employed before the OFDM modulation. The equivalence between CDD and PD is obvious because of the properties of the Discrete Fourier Transform (DFT). It can be derived from the definition of the IDFT:

$$s(l) = \frac{1}{\sqrt{N_F}} \cdot \sum_{k=0}^{N_F-1} S(k) \cdot e^{j\frac{2\pi}{N_F}kl} \tag{12}$$

$$\underbrace{s((l-\delta_{cy}) \bmod N_F)}_{\text{CDD signal}} = \frac{1}{\sqrt{N_F}} \cdot \sum_{k=0}^{N_F-1} \underbrace{e^{-j\frac{2\pi}{N_F}k\cdot\delta_{cy}} \cdot S(k)}_{\text{PD signal}} \cdot e^{j\frac{2\pi}{N_F}kl}. \tag{13}$$

In order to achieve diversity effects for the OFDM system with bandwidth W the delay δ_n has to fulfil the following condition:

$$\delta_n \geq \frac{1}{W}, \qquad n = 1, \ldots, N-1. \tag{14}$$

As a consequence of the use of OFDM with CDD the frequency selectivity is increased, whereas the coherence bandwidth is decreased [5].

3.2 Effects of Cyclical Delay Diversity

In this section we want to deal with the effects and results of the usage of OFDM in combination with multiple antennas and CDD. Therefore we first have a look at

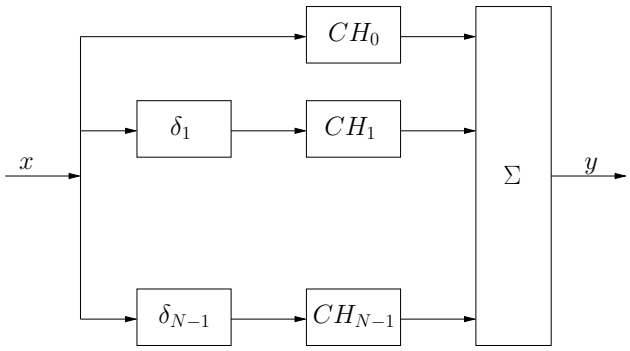

Figure 11: DD channel model

the uncoded transmission and the transformation of the channel. Then we investigate the resulting bit error curves with and without coding and study why only coded transmission can take advantage of the inserted diversity. Finally we will investigate the influence of an additional interleaver on the system performance.

3.2.1 Uncoded transmission with OFDM and CDD

First of all we have to have a look at the effects of the spatial antenna diversity. For simplicity we just concern Delay Diversity which can be easily evaluated to point out the main ideas behind this diversity concept. In figure 11 the channel model for DD is shown. The channel output *y* can be calculated from the input sequence *x* as follows:

$$\begin{aligned} y(k) &= x(k) * H_{CH_0} + x(k) * \delta(k-\delta_1) * H_{CH_1} + \ldots + x(k) * \delta(k-\delta_{N-1}) * H_{CH_{N-1}} \\ &= x(k) * \underbrace{\left(H_{CH_0} + \delta(k-\delta_1) * H_{CH_1} + \ldots \delta(k-\delta_{N-1}) * H_{CH_{N-1}}\right)}_{H_{eq}} \\ &= x(k) * H_{eq}, \end{aligned}$$

where H_{CH_i} and H_{eq} denotes $H_{CH_i}(k,\kappa)$ and $H_{eq}(k,\kappa)$, respectively and $*$ the convolutional product. We notice that the time-variant subchannels $H_{CH_i}(k,\kappa)$ are transformed in an equivalent channel $H_{eq}(k,\kappa)$ with additional virtual paths introduced by the different antenna specific delays (virtual echos).

To demonstrate the transformation we want to have a closer look on a one path time-variant channel namely the Rayleigh channel. There we expect to get most influence of multiple antennas.

In figure 12 the error distribution of a two antenna system over 64 OFDM carriers is plotted. Each dot in the plot represents an error in the uncoded transmission

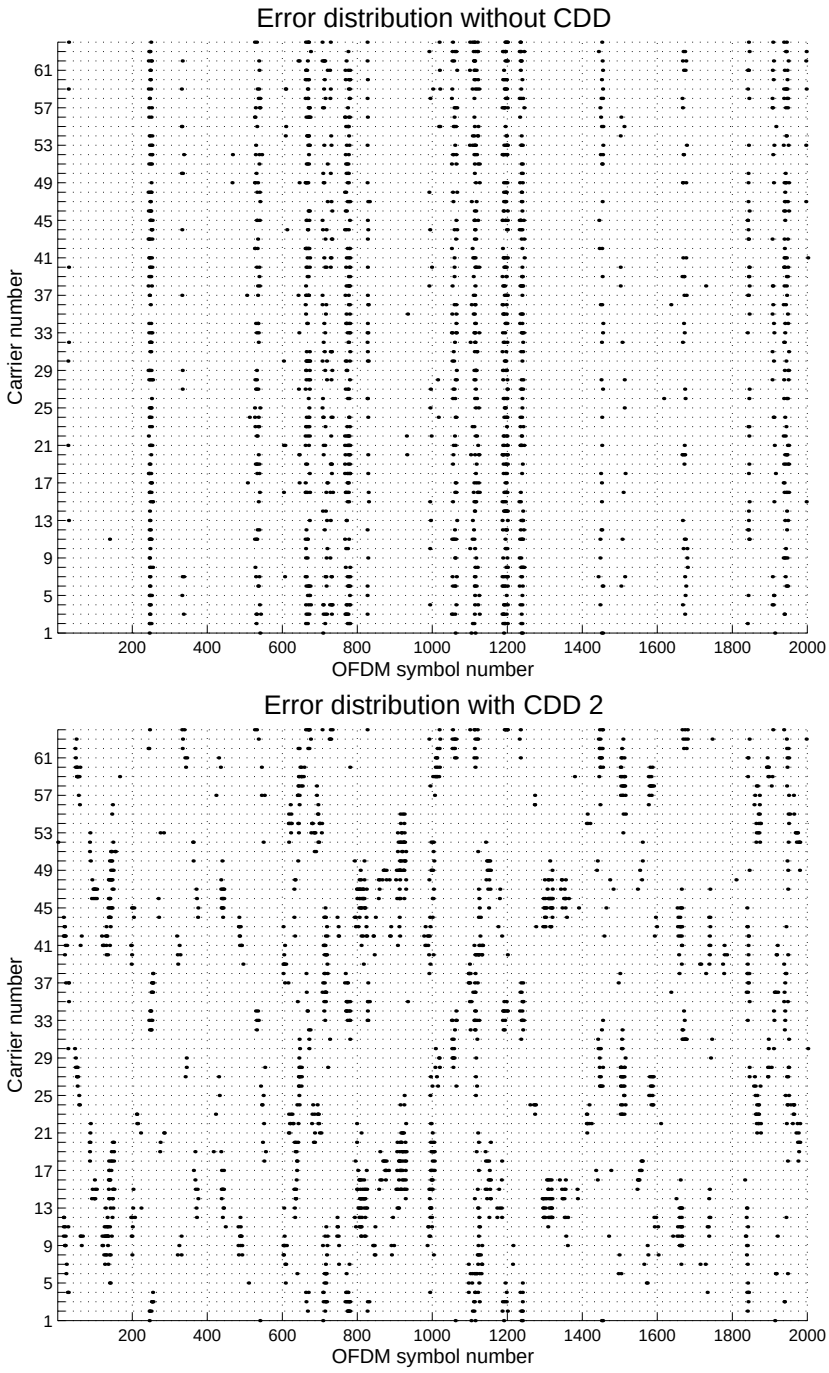

Figure 12: Rayleigh channel with 2 Tx and no shift (top) and CDD shift 2

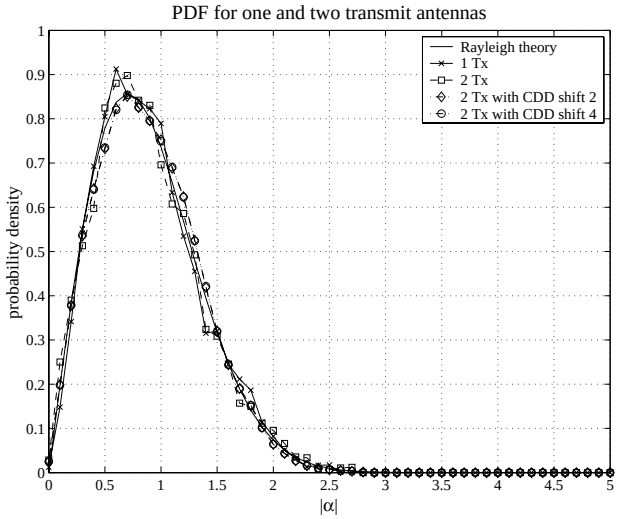

Figure 13: Probability density function (PDF) for one and two transmit antennas

with hard decision (half-plane decision for BPSK). The upper scatter diagram corresponds to a system without cyclic shift and shows flat-fading characteristics typical for the one path Rayleigh channel. Whereas the lower plot shows the same system with CDD and a shift of 2 samples. Here we notice frequency selective fading, but the number of errors is approximately the same. Therefore only the error pattern differs significantly between CDD and an unshifted system but not the number of errors.

In figure 13 the probability density function (PDF) is plotted. It is almost identical for one and two transmit antennas even with different cyclic shifts. The horizontal axe is marked with $|\alpha|$ which denotes the absolute value of the channel estimation. All curves show the same Rayleigh characteristics. Therefore and because of the preceding investigations we expect the different uncoded transmissions (concerning the number of antennas, use of CDD and number of shifts) to show almost equal performance.

In figure 14 the bit error rate (BER) is plotted over the signal-to-noise ratio (SNR) of the complex additive white gaussian noise (AWGN). The previous expectation is shown because all schemes yield to roughly the same BER. We can draw the conclusion that we have to do some extra efforts to take advantage out of the additional diversity. OFDM with CDD itself is not capable to use it.

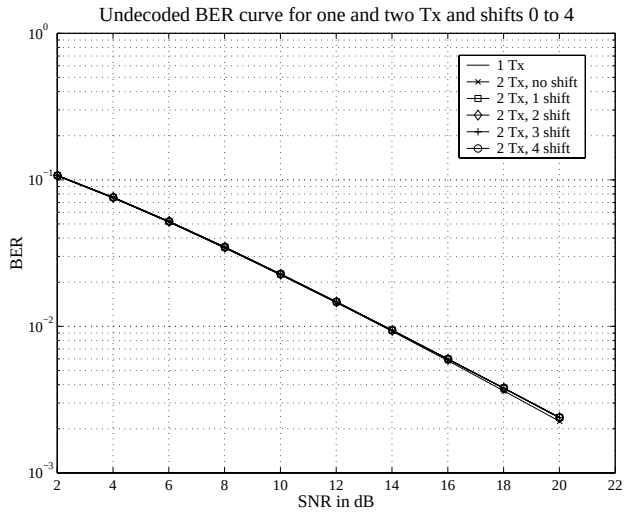

Figure 14: Bit error rate (BER) for one and two transmit antennas

3.2.2 Influence of additional convolutional coding

From the last section we can already draw the conclusion that CDD mainly changes the error distribution. A Rayleigh channel, which can be approximated by the Gilbert-Elliot model, is then transformed into a frequency selective multipath channel as shown in the previous section. Here we only want to investigate the effects of convolutional coding and the achievable gains.

In figure 15 we see the BER curve over the SNR for a two transmit antenna CDD system and cyclic shifts from no shift up to four samples. We notice that with an increasing shift we can achieve better performance. Most gain can be reached with the step from no shift to one sample. The improvements from one to the next then decreases with each step.

For further investigations on the effects of CDD and the difference to an unshifted system we have to introduce some definitions:

Code C is a binary convolutional code with rate $R = b/c$ encoded by a rational generator matrix $G(D) = [g_{ij}]$, $i = 1,\ldots,b$ and $j = 1,\ldots,c$. The information sequence $u(D) = u_0u_1\ldots$ with $u_i = u_i^0\ldots u_i^{b-1}$ is encoded to the code sequence $v(D) = v_0v_1\ldots$ with $v_j = v_j^0\ldots v_j^{c-1}$. m denotes the encoder memory and ν_{min} the minimal constraint length [9].
The encoder state σ is the content of the memory elements of an encoder with a generator matrix $G(D)$. The set of encoder states $S = \{0,1,\ldots,2^\mu - 1\}$ is called the encoder state space. $\sigma = 0$ corresponds with all memory elements to be zero.

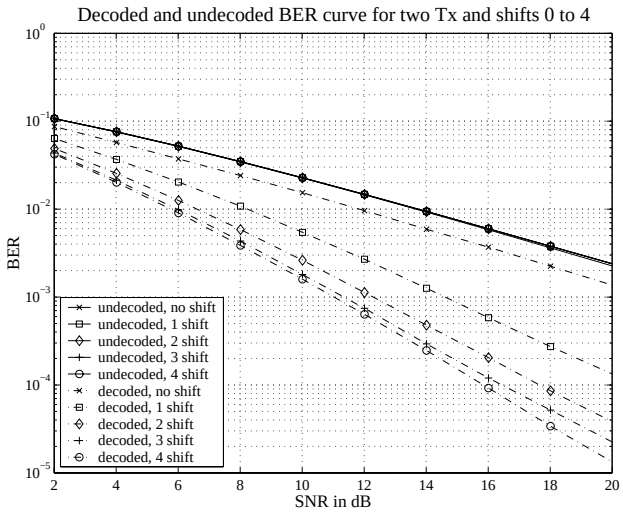

Figure 15: Bit error rate (BER) for 2 Tx and different cyclic shifts ($v = 200$ km/h)

$S^{\sigma_s,\sigma_e}_{[t_1,t_2]}$ denotes the set of encoder states $\sigma_{[\sigma_{t_1}\sigma_{t_2}]} = \sigma_{t_1}\sigma_{t_1+1}\ldots\sigma_{t_2}$ starting at state $\sigma_s = \sigma_{t_1}$ and ending at state $\sigma_e = \sigma_{t_2}$. Besides $\sigma_{[\sigma_{t_1}\sigma_{t_2}]}$ must not have the state transition from zero to zero state ($\sigma_i = 0$, $\sigma_{i+1} = 0$ for $t_1 \leq i \leq t_2 - 1$).

Now we can define the j-th order active burst distance [8]:

$$a^b_j = \min_{S^{0,0}_{[0,j+1]}} \{wt(v_{[0,j]})\}, \tag{15}$$

where $j \geq \nu_{min}$ and $wt(\cdot)$ denotes the (Hamming) weight of the sequence. The active burst distance is an encoder property and it is undefined for $j < \nu_{min}$. Further it can be used to determine how many errors in a code word window of size j are necessary so that there might occur an error.

Let $e_{[k,l)} = e_k e_{k+1}\ldots e_{l-1}$ denote the error pattern ($e_l = 0 \Rightarrow$ correct position, $e_l = 1 \Rightarrow$ erroneous position). A convolutional code C can correct any incorrect segment between two correct states σ_{t_1} and σ_{t_2} if the error pattern $e_{[t_1,t_2)}$ satisfies the following condition [7]:

$$wt(e_{[t_1+k,t_1+1+i)}) < \frac{a^b_{i-k}}{2} \tag{16}$$

for $0 \leq k \leq t_2 - t_1 - \nu_{min} - 1$, $k + \nu_{min} \leq i \leq t_2 - t_1 - 1$.

Now let us concern a convolutional code with a code word size of one OFDM symbol. With equation (16) we can now give a prediction how many undecoded

errors can definitively be corrected by the decoder. If the error pattern within one OFDM symbol does not fulfil the equation above a decoder failure might occur. On the other hand if the error pattern passes this test we can definitively be sure that the decoder is able to correct the errors. Therefore we can now investigate the error distribution in a code word and furthermore make an assertion whether the error pattern will lead to an error or not.

In our example we use the optimum free distance $(5,7)_{oct}$ convolutional code with memory $m = 2$, $\nu_{min} = 2$ and $d_{free} = 5$. Therefore we can always correct at least

$$t = \left\lfloor \frac{d_{free} - 1}{2} \right\rfloor = 2 \tag{17}$$

errors [3]. In figure 16 the histogram of the errors in a code word for a two transmit antenna system with and without CDD is plotted. We transmit 10000 terminated codewords with the code mentioned above of length 64 which corresponds with the used OFDM symbol length. Therefore we fulfil the criteria given in equation (16): $\sigma_{t_1} = 0$ and $\sigma_{t_2} = 0$ are fixed because the Viterbi algorithm can force these border states. As calculated in equation (17) we can correct at least two errors and therefore we are only interested in codewords with more than two errors which can lead to decoder failures. Besides we can differentiate, whether the error pattern of higher weight will produce errors or not.

In figure 16 we notice the difference between CDD and an unshifted transmission. Last mentioned shows many error-free code words but on the other hand also many packets with higher weighted error patterns leading to even more errors in the decoded result. This is characteristic because of the flat-fading behaviour of the Rayleigh channel which can be seen in figure 12, too. Whereas CDD results in more single or double errors per code word. But as we already noticed this does not really challenge the convolutional decoder because it can always correct them. Besides there are much less high weighted error patterns, which negatively affect the correction performance, compared to the unshifted transmission. Further we have to mention that the figure is cut at 700 symbols for presentability reasons.

Summarising we can note that CDD does not change the number of uncoded bit errors significantly compared with the unshifted transmission but instead it introduces some kind of virtual paths which can break the flat fades. This causes an increased frequency selectivity. Further it increases the lower weighted error patterns and decreases the higher weighted so that the overall number of errors remains approximately constant. Normally this improves the performance of a convolutional decoder which is better suited for widespread error patterns. The typical error patterns of the Rayleigh channel are periods with on the one hand almost no errors (only AWGN) and on the other hand with many errors ($P_B \to 0.5$). There the convolutional decoder will fail.

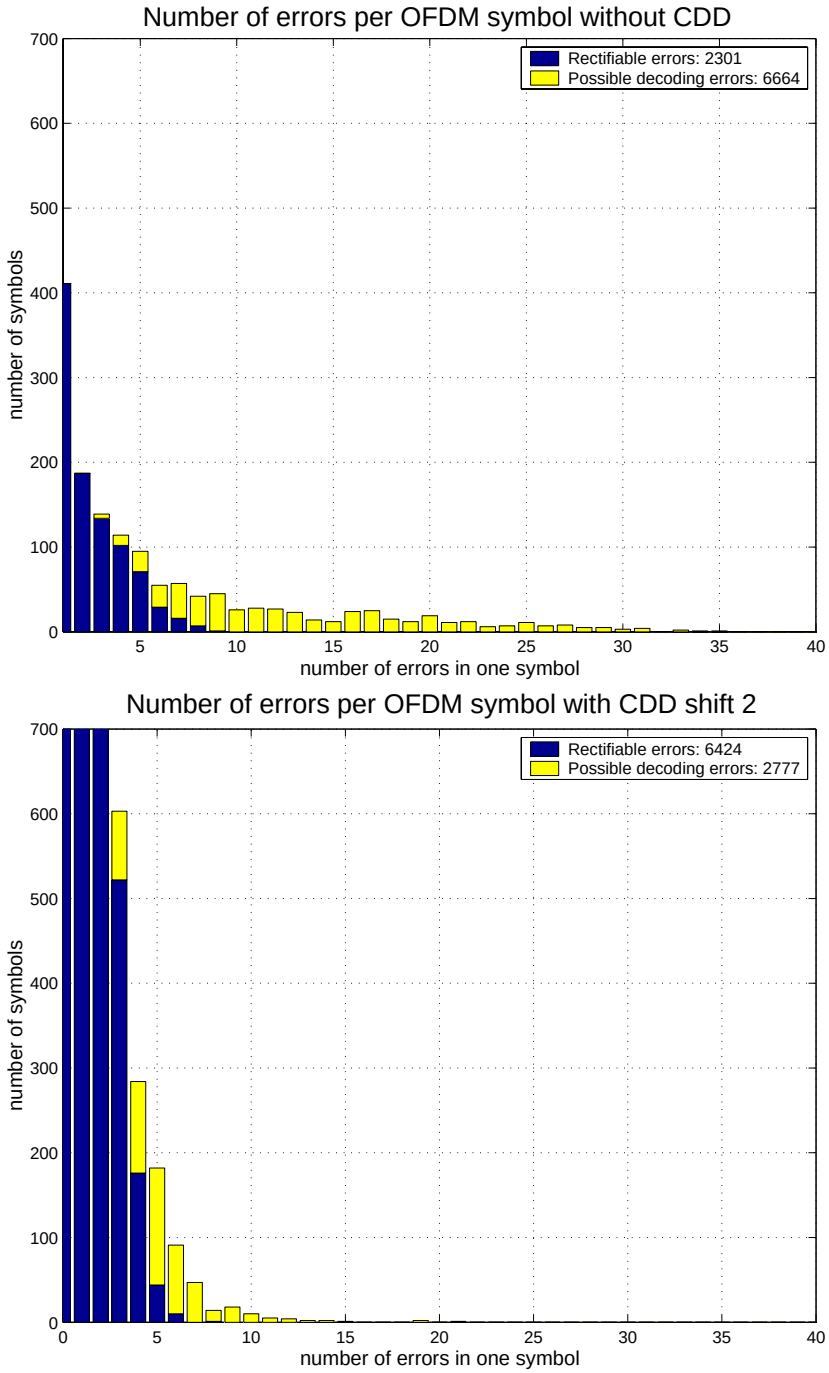

Figure 16: Number of bit errors in code words at length 64 of a $(5,7)_{oct}$-convolutional code at a SNR=12dB

3.2.3 Comparison with interleaving

As we found out in the last section the results attainable with CDD are mainly based on the redistribution of erroneous bits. Therefore it poses the question, if we can reach the same effects with an interleaver. Its purpose is to spread the errors over many OFDM symbols in order to transform flat-fading in preferably (for the decoder) uncorrelated error patterns. It is well known that these performance improvements are possible. Therefore we want to concentrate here more on the window length of the interleaver needed to reach comparable results. Of course this is strongly tied with the used channel and here especially with the speed of variation. The interleaver window has to be larger than the length of a fade to obtain advantages because there is no sense in permuting erroneous bits.

Now we want to compare a single antenna system with different interleaver sizes with a two antenna system with CDD. This constellation was chosen because we want to weigh between the best results achievable with an additional antenna and a system without these efforts but with supplementary software methods. In the simulation always a velocity of $v = 200$ km/h was set. For slower speeds the channel changes slower and we need a larger interleaver to guarantee that the window is longer than the fades.

In figure 17 an one antenna OFDM system with a random interleaver and window sizes ranging from 10 to 100 and a two antenna system with CDD and a cyclic shift of 4 over a Rayleigh channel are compared. For both systems a velocity of 200 km/h is set. For lower SNR (up to 10dB) we observe that CDD achieves approximately the same performance as an interleaver with window length of 40 OFDM symbols which is equal to $40 \cdot 64 = 2560$ samples. But we also notice that the comparison between the performances of CDD and the interleaver length depends on the used SNR. The CDD curve has a sharper decline for higher signal to noise ratios and therefore the curves diverge.

In figure 18 this problem is plotted in more detail. The interleaver window is increased from 10 to 80 OFDM packets (each has 64 samples). Those results for four different signal to noise ratios are shown and for comparison the appropriate value for CDD shift 4 is given. The curves for the interleaver decline for larger windows because the error pattern can be spread over a wider range. We notice that for an increasing SNR the intersection of the interleaver curve and the BER of CDD moves towards longer window sizes. Now we can make a trade off between the delay caused by interleaving and the additional effort for a second transmit antenna.

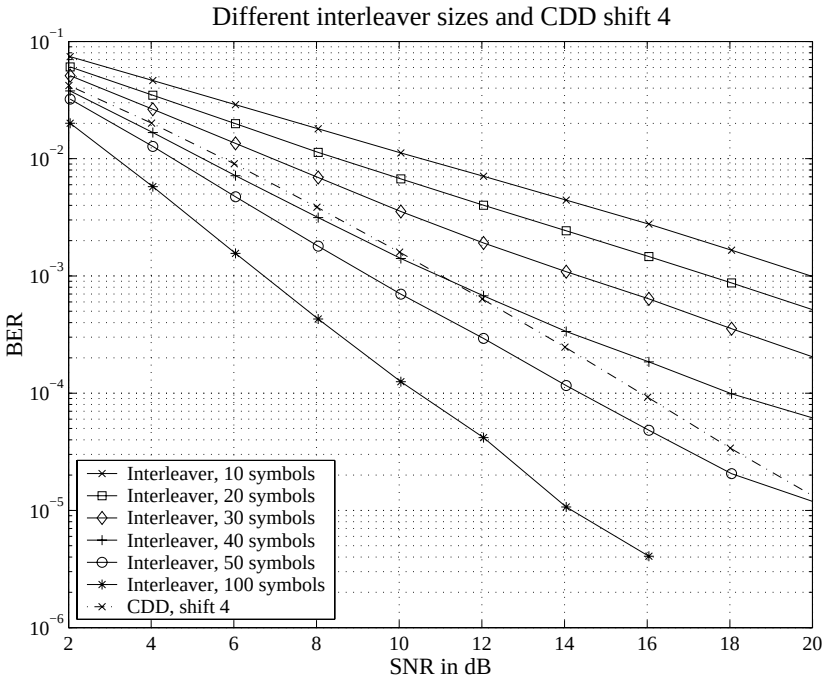

Figure 17: Comparison of a random interleaver with CDD

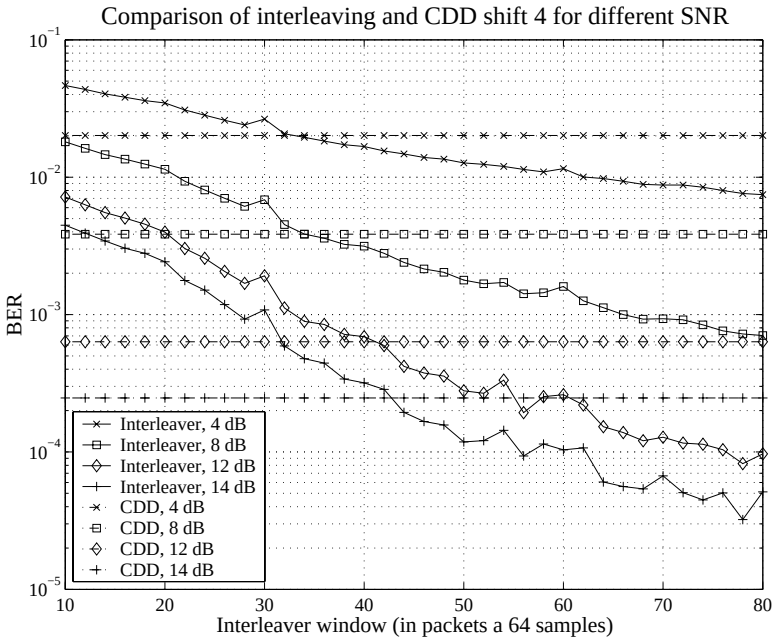

Figure 18: Different interleaver windows and CDD with shift 4

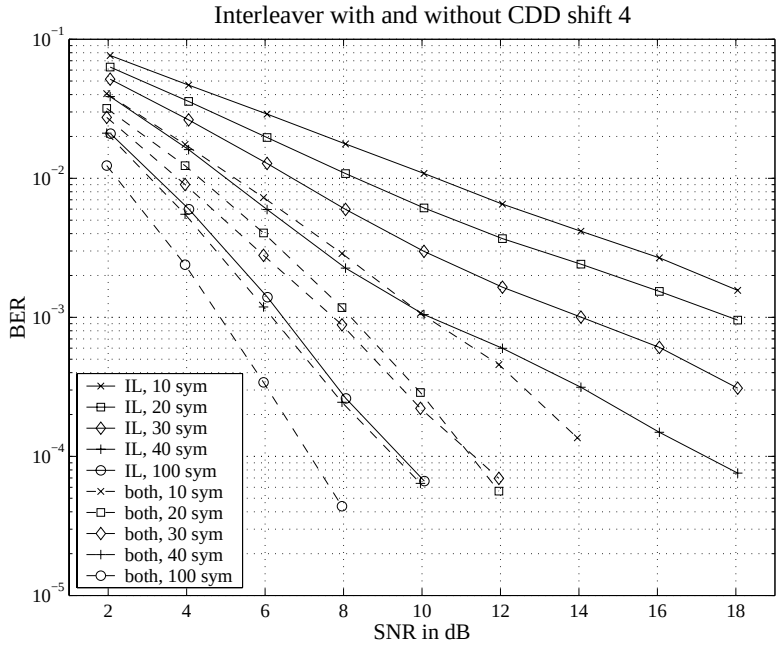

Figure 19: Combination of interleaver and CDD in comparison to a single antenna transmission with interleaving

3.2.4 Combination of CDD and interleaving

Another point of interest is the combination of the methods mentioned above. As both are only based on the destruction of error bursts by lowering the error density we expect a lower gain for long interleaver windows. In figure 19 this proves to be valid. For small values we can improve by approximately 9dB whereas for interleaving over 100 OFDM symbols we obtain a melioration of only about 2dB. Therefore we can mitigate the undesired delay introduced by interleaving using smaller windows and in exchange cyclic delay diversity (CDD).

Another interesting aspect is the possibility of using an interleaver and OFDM without an additional delay. Of course this is not possible in general. But if we concern it in connection with the serial-to-parallel conversion which is necessary for OFDM and therefore restrict the interleaver length to one OFDM symbol the above mentioned thesis gets reasonable. In figure 20 the random interleaved and Viterbi decoded version is compared with a non-interleaved for a Rayleigh channel and CDD with a cyclic shift of 4 samples. We notice for the non-interleaved transmission that for an increasing number of carriers we have worse performance. This results from the additional carriers which have to share the same bandwidth

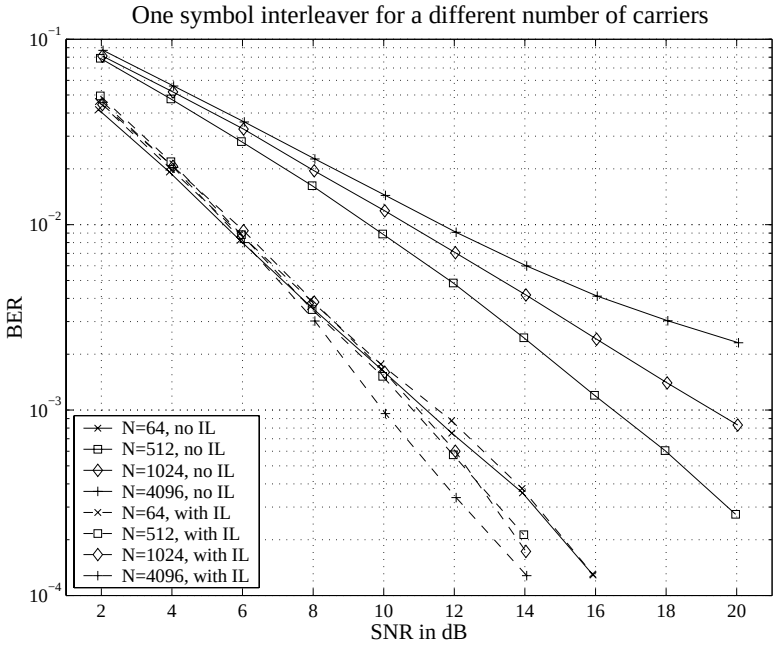

Figure 20: Interleaving over one OFDM symbol for different number of carriers and CDD shift 4

(necessary for a fair comparison). Therefore we encounter interferences deteriorating the bit error rate. They can be made visible by looking at the received and equalised samples. For $N_F = 64$ we have almost only complex points close around ± 1 (BPSK modulation), whereas for $N_F = 4096$ we also have them in the opposite plane which leads to bit errors even without AWGN. On the other hand it is preferable to use more carriers so that the interleaver performs better. For low N_F there is almost no difference between both versions because the interleaver cannot distribute the error patterns sufficiently. For longer symbol lengths we can take advantage out of the frequency selectivity which CDD introduces to the Rayleigh channel. An unshifted transmission scheme would not be able to do this because during a flat-fade we could only permute erroneous bits. While being in a good channel state we almost only face uncorrelated AWGN which can not be improved by interleaving. But with the additional effort we can obtain equal or even better performance. Therefore its use is advisable especially when many carriers and no outer interleaver can be used.

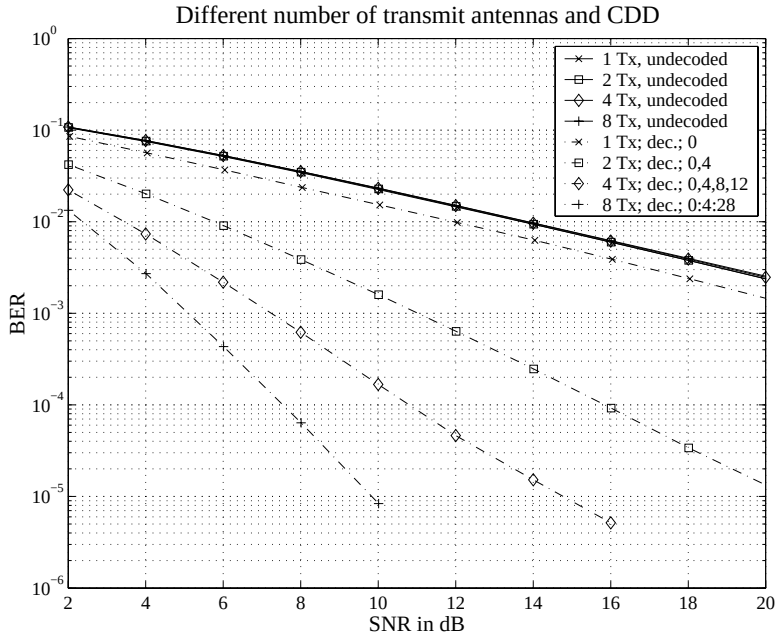

Figure 21: Performance of different number of transmit antennas over a Rayleigh channel

3.2.5 Performance on realistic channels and multiple antennas

Sometimes it is desirable to further increase the spatial antenna diversity to obtain better transmission characteristics. In figure 21 the bit error curves for one, two, four and eight transmit antennas over a Rayleigh fading channel are plotted. On each antenna an additional cyclical shift of four is performed to get the corresponding diversity for the antenna. As supposed we achieve best performance with eight antennas. The uncoded transmission characteristics for different number of transmit antennas are similar because of the Rayleigh distribution of the channel values which stay unchanged. Only with coding we can bring out the inserted diversity. The signal-to-noise gain for more antennas decreases with each additional antenna.

So far we have only investigated the behaviour of CDD for a one path Rayleigh fading channel. In reality we often face the problem of multi-path propagation. In table 1 we have the parameters of an exemplary six path WSSUS channel model.

In figure 22 the corresponding BER curves for different shifts is depicted. As already noticed before we know that CDD increases the frequency selectivity (confer to figure 12). In this case we do not transmit over a flat-fading channel

delay in samples	0	1	2	3	6	10
relative power	1.0	0.81	0.54	0.44	0.35	0.19
Rice factor	0	0	0	0	0	0
Fixed Doppler shift	0	0	0	0	0	0

Table 1: Six path Wide Sense Stationary Uncorrelated Scattering (WSSUS) channel used for simulation

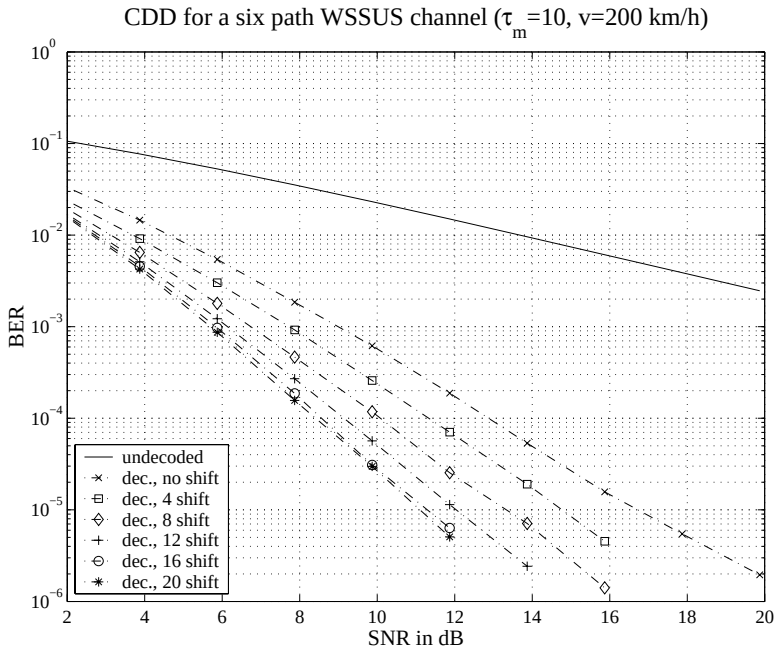

Figure 22: Performance of CDD for a multi-path channel

as before but we have variance also in frequency direction. Therefore we expect CDD to have less influence on the BER performance compared to the one path model. Figure 22 shows this for cyclic shifts of 0, 4, 8, 12, 16 and 20. We can only gain about 2 dB with the step from shift 0 to 4. With further steps the additional amelioration decreases as already observed for the one path model.

3.3 Conclusion

Comprising we can say that CDD over OFDM absolutely needs a higher-ranked decoder which uses the inserted diversity and is able to take advantage out of the lowered error density in fades respective the permutation of the error pattern on

the output. The BER with and without cyclic shift are identical (figures 13 and 14). But CDD introduces additional frequency selectivity (figure 12) which breaks for example the flat-fading of a Rayleigh channel. This enables us to use an one symbol interleaver to distribute the errors over the whole symbol. Especially for many carriers this is advisable. Another possibility is to use an interleaver over some OFDM symbols instead of CDD. Then we can save an additional antenna but we have to deal with other problems namely the unpreventible time delay. Besides we lose the higher robustness against an antenna failure. It has been shown that even the combination of interleaver and CDD may improve the performance. This effect reduces for larger windows. Finally the results for more realistic mobile communication channels were investigated. Here the differences between CDD and an unshifted transmission decrease because the gain from one path to a (virtual) second path is the highest. The same constellations appears for multiple antennas. Here we have the highest effect for the step from one to two. Afterwards the additional gain reduces with each step.

4 The Alamouti scheme and OFDM

As we already noticed in the previous section we can achieve better BER performance using spatial diversity, e.g., with multiple transmit antennas. Now we want to investigate another scheme proposed by Alamouti [1]. It provides the possibility to use two transmit antennas and multiple receive antennas but here we only want to consider the case of transmit diversity. Further it can be generalised to more than two antennas but only with two we can get the full diversity without loss of transmission rate [20].

4.1 The Alamouti transmit diversity scheme

Alamouti proposed a new transmission scheme for two transmit antennas and multiple receive antennas which take advantage out of the additional diversity of the space direction. Therefore we do not need extra bandwidth or redundancy in time or frequency direction. We can use this diversity for example to get a decreased sensitivity to fading and can achieve a better bit error rate or use higher level modulation.

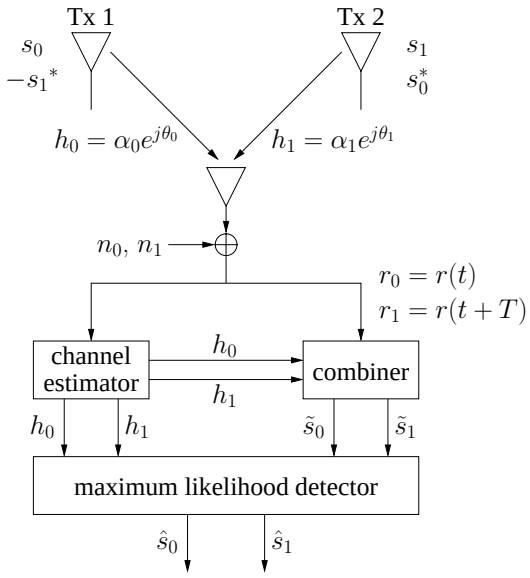

Figure 23: The Alamouti transmit diversity scheme

We assume a transmission system as illustrated in figure 23. On both transmit antennas Tx 1 and Tx 2 we transmit the information symbols s_0 respective s_1

	Tx 0	Tx 1
time t	s_0	s_1
time $t+T$	$-{s_1}^*$	s_0^*

Table 2: Alamouti's transmission scheme for the information symbols s_0 and s_1

simultaneously according to the scheme in table 2 where T denotes the symbol duration and t the respective time slot.

Here we only want to investigate the system mentioned above with one receive antenna. Therefore we obtain two channel responses which have to be uncorrelated to achieve best results. Experimental results have shown that two transmit antennas have to be about ten wavelengths apart to provide sufficient decorrelation. To get the same results on the remote side only a distance of approximately three wavelength is needed. This results from the supposed vicinities of the base station and the mobile device which are normally different. For the mobile station nearby scatterer are assumed. This assumption cannot be made for the base station because characteristic for it is the placing on a higher altitude. Besides the average power of the two antennas should not differ more than 3dB [1].

We now model the channel as a complex multiplicative distortion composed of a magnitude and a phase component. The channel from Tx 1 to the receive antenna is characterised by h_0 and analogously for Tx 2 we get h_1:

$$\begin{aligned} h_0 &= \alpha_0 \cdot e^{j\theta_0} \\ h_1 &= \alpha_1 \cdot e^{j\theta_1}. \end{aligned} \tag{18}$$

Further we assume that fading is constant over two consecutive symbols. Therefore we write $h_0 = h_0(t) = h_0(t+T)$ respective $h_1 = h_1(t) = h_1(t+T)$. In practical realisations we can handle this assumption by using e.g. the average of the two channel impulse response values. We expect to minimise therewith the estimation error for both symbols. On the receiver side we get two symbols $r_0 = r(t)$ and $r_1 = r(t+T)$:

$$\begin{aligned} r_0 &= h_0 s_0 + h_1 s_1 + n_0 \\ r_1 &= -h_0 s_1^* + h_1 s_0^* + n_1. \end{aligned} \tag{19}$$

The variables n_0 and n_1 denote complex white gaussian noise from the receiver and from interferences.

In the receiver we have the following blocks:

- *Channel estimator*: In this work and in the simulations we assume perfect knowledge of the channel. In real systems this has to be done using for example pilot symbols where known symbols are transmitted periodically. The receiver can then estimate the channel and interpolate the unknown positions. Possible errors are especially the time variance, wrong interpolation caused by e.g. narrow-band distortion or quantisation effects. Besides the pilot insertion frequency has to be higher than the Nyquist sampling rate to minimise the channel estimation error [1].

- *Combiner*: It uses the received symbols r_0 and r_1 with the results from the channel estimator h_0 and h_1 to calculate the following two combined signals $\tilde{s}_0$ and $\tilde{s}_1$:

$$\begin{aligned} \tilde{s}_0 &= h_0^* r_0 + h_1 r_1^* \\ \tilde{s}_1 &= h_1^* r_0 - h_0 r_1^*. \end{aligned} \tag{20}$$

  Using equations (18) and (19) substituting the appropriate variables in equation (20) we get:

$$\begin{aligned} \tilde{s}_0 &= \left(\alpha_0^2 + \alpha_1^2\right) \cdot s_0 + h_0^* n_0 + h_1 n_1^* \\ \tilde{s}_1 &= \left(\alpha_0^2 + \alpha_1^2\right) \cdot s_1 - h_0 n_1^* + h_1^* n_0. \end{aligned} \tag{21}$$

- *Maximum likelihood detector*: Using the above equations we can calculate the decided symbol $\hat{s}_0$. Choose s_i if

$$\left(\alpha_0^2 + \alpha_1^2 - 1\right) |s_i|^2 + d^2\left(\tilde{s}_0, s_i\right) \leq \left(\alpha_0^2 + \alpha_1^2 - 1\right) |s_k|^2 + d^2\left(\tilde{s}_0, s_k\right) \quad \forall\, i \neq k \tag{22}$$

  with $d^2(x, y) = (x - y) \cdot (x^* - y^*)$.

  For PSK all symbols have the same energy ($|s_i|^2 = |s_k|^2 = E_s, \forall\, i, k$). Therefore equation (22) simplifies to

$$d^2\left(\tilde{s}_0, s_i\right) \leq d^2\left(\tilde{s}_0, s_k\right) \quad \forall\, i \neq k. \tag{23}$$

  For $\hat{s}_1$ equation (22) and (23) can be derived analogously.

An advantage of the Alamouti scheme is the added reliability against the failure of one antenna. For example if Tx 2 as illustrated in figure 23 fails we receive only signals from Tx 1 and therefore $h_1 = 0$. We get:

$$\begin{aligned} r_0 &= h_0 s_0 + n_0 \\ r_1 &= -h_0 s_1^* + n_1. \end{aligned} \tag{24}$$

The Combiner then provides the following values to the maximum liklihood detector:

$$\begin{aligned} \tilde{s}_0 &= h_0^* r_0 = \alpha_0^2 s_0 + h_0^* n_0 \\ \tilde{s}_1 &= -h_0^* r_1^* = \alpha_0^2 s_1 - h_0 n_1^*. \end{aligned} \tag{25}$$

We notice that the combined signals are equal to the transmission without diversity. The diversity gain is then lost but we can still transmit [1].

Another important issue we have not considered yet is soft decoding. This means that we do not simply hard decide to bits but also include reliabilities for each bit position. Schulze [18] therefore proposed a possibility to calculate the log-likelihood ratio for each bit. We receive from the channel the two complex values r_0 and r_1 which leads to the vector $\mathbf{r}$ consisting of r_0 and the complex conjugated of r_1. Further we have the channel matrix $\mathbf{C}$ obtained from the impulse responses of the two transmit antennas to the receive antenna $h_0 = h_0(t) = h_0(t+T)$ and $h_1 = h_1(t) = h_1(t+T)$. Suppose we have transmitted the vector $\mathbf{s}$ with two complex symbols s_0 and s_1 then we can describe the transmission with Alamouti's scheme as follows:

$$\underbrace{\begin{pmatrix} r_0 \\ r_1^* \end{pmatrix}}_{\mathbf{r}} = \underbrace{\begin{pmatrix} h_0 & h_1 \\ h_1^* & -h_0^* \end{pmatrix}}_{\mathbf{C}} \cdot \underbrace{\begin{pmatrix} s_0 \\ s_1 \end{pmatrix}}_{\mathbf{s}} + \underbrace{\begin{pmatrix} n_0 \\ n_1 \end{pmatrix}}_{\mathbf{n}}. \tag{26}$$

The optimum receiver has then to evaluate the squared euclidian distance

$$\hat{x} = \arg\min_{\mathbf{s}\,\varepsilon\,S} \| \mathbf{r} - \mathbf{C}\mathbf{s} \|^2, \tag{27}$$

where S is the set of all possible transmit symbol combinations. The arg operation assigns the appropriate sent vector to $\hat{x}$. The equation comes from the maximum likelihood principle, where the most probable transmission symbol vector $\mathbf{s} = (s_0,\, s_1)^T$ minimises the squared euclidian distance. Last mentioned is defined as $\| (x,\, y)^T \| = \sqrt{|x|^2 + |y|^2}$.

Each transmit vector $\mathbf{s}$ corresponds to a vector $\mathbf{b} = (b_1, \ldots, b_m)$ of binary digits. Therefore we can now give the log-likelihood ratio for bit b_i with $i = 1, \ldots, m$ under the condition of the received vector $\mathbf{r}$:

$$\Lambda(b_i|\mathbf{r}) = \ln \left(\frac{\sum_{\mathbf{s}\,\varepsilon\,S_i^{(0)}} \exp\left(-\frac{1}{2\sigma_n^2} \| \mathbf{r} - \mathbf{C}\mathbf{s} \|^2 \right)}{\sum_{\mathbf{s}\,\varepsilon\,S_i^{(1)}} \exp\left(-\frac{1}{2\sigma_n^2} \| \mathbf{r} - \mathbf{C}\mathbf{s} \|^2 \right)} \right). \tag{28}$$

$S_i^{(0)}$ is the set of transmitted signals $\mathbf{s}$ with $b_i = 0$ and $S_i^{(1)}$ analogously for $b_i = 1$. $\ln(\cdot)$ denotes the natural logarithm and $\sigma_n^2 = N_0/2$ is the variance of the additive gaussian noise with noise power N_0 of the channel.

Of course we can also use the calculation result to make hard decision:

$$\Lambda(b_i|\mathbf{r}) \text{ is } \begin{cases} > 0 & \text{for } b_i = 0 \\ < 0 & \text{for } b_i = 1 \end{cases}. \tag{29}$$

For high SNR values (= small σ_n^2) we get numerical problems with equation (28). In [19] and [17] a possibility for a stable evaluation is proposed:

$$\ln\left(e^{\delta_1} + e^{\delta_2}\right) = \max(\delta_1,\, \delta_2) + \ln\left(1 + e^{-|\delta_2 - \delta_1|}\right). \tag{30}$$

In general we can express the problem as follows:

$$\delta^{(m-1)} = \ln\left(e^{\delta_1} + \ldots + e^{\delta_{m-1}}\right) \tag{31}$$

and then we obtain

$$\begin{aligned} \ln\left(e^{\delta_1} + \ldots + e^{\delta_m}\right) &= \ln\left(e^{\delta^{(m-1)}} + e^{\delta_m}\right) = \\ &= \max(\delta^{(m-1)},\, \delta_m) + \ln\left(1 + e^{-|\delta_m - \delta^{(m-1)}|}\right). \end{aligned} \tag{32}$$

One assumption of the Alamouti scheme is that the channel impulse response must not change during two consecutive symbols. One solution to cope with this problem is to take the channel values $h_0(t)$ and $h_0(t+T)$ respective $h_1(t)$ and $h_1(t+T)$ and to calculate the respective average. This was already mentioned above. But therewith we face the problem, that neither for the first symbol nor for the second one the correct channel value is taken. The error is only spread over both symbols. Therefore we loose information about the channel. This becomes more and more noticeable for higher velocities of the mobile receiver which equals with a faster fading channel.

With the approach of Schulze we can avoid this problem. The Alamouti decoding process is shifted in the channel matrix $\mathbf{C}$ (confer to equation (26)). We notice, that the upper row of the matrix affects only the symbols s_0 and s_1 at time t. Whereas the second row influences the transmit symbols $-s_1^*$ and s_0^* at time $t+T$. In contrast to Schulze we take different channel values $h_0(t)$ and $h_1(t)$ respective $h_0(t+T)$ and $h_1(t+T)$ for the two time slots (= rows of the channel matrix $\mathbf{C}$). Therefore we utilise the estimation for each of the two channels from transmitter to the receiver and now additionally for each time slot. All information available from the channel estimation is used. This leads to a new channel matrix:

$$\mathbf{C} = \begin{pmatrix} h_0(t) & h_1(t) \\ h_1^*(t+T) & -h_0^*(t+T) \end{pmatrix}. \tag{33}$$

The following decoding process stays unchanged. An implementation drawback is the necessity to keep all channel values in memory. The old scheme requires only half of them. The results of these changes are investigated in subsection 4.4.

Since now Alamouti's scheme is not adapted to the special case of underlying OFDM. In the following subsections we present two implementation possibilities. The first is the *Space-Time* transmission and the other is the *Space-Frequency* transmission. Both will be introduced in the following subsections.

4.2 Space-Time transmission

It is well known that OFDM transforms WSSUS channels into N_F subchannels which show Rayleigh fading characteristic [6]. This is well suited for the Alamouti scheme.

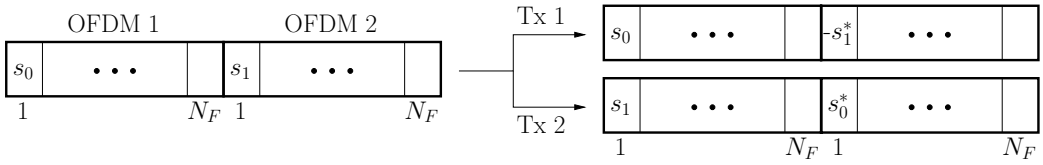

Figure 24: Principle of Alamouti Space-Time coding over OFDM

In figure 24 the principle of the Space-Time Code (STC) implementation is illustrated according to table 2. First the information bits are modulated with a suited modulation alphabet A_x. Then the symbol sequence is divided into blocks each with N_F symbols. We take always the i-th symbol with $1 \leq i \leq N_F$ of two successive blocks. Therefore the number of blocks has to be a multiple of 2. The first symbol corresponds with s_0 the second with s_1. Then we split the sequence into two streams for the two antennas. On the i-th position of the first block of the first antenna we put s_0 and on the i-th position of the second block $-s_1^*$. Analogously we perform this for the second antenna with s_1 respective s_0^*. Afterwards each Alamouti encoded stream of blocks is transmitted using OFDM.

Assuming an AWGN channel we would therefore receive the i-th symbol of the first block after the OFDM decoding as $r_0 = s_0 + s_1 + n_0$. For the second block this would be $r_1 = -s_1^* + s_0^* + n_1$.

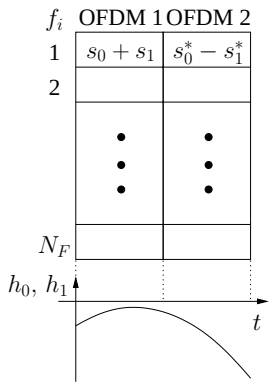

Figure 25: Problems of Space-Time coding over OFDM

One assumption of the original Alamouti scheme is, that fading should be constant during two consecutive and related symbols s_0 and $-s_1^*$ respective s_1 and s_0^*. This means that the channel must not change over two OFDM symbols. As shown in figure 25 the disadvantage of this implementation is the increased sensitivity against fast fading. On the other hand we gain from the increased robustness against frequency selective fading coming from multi-path channels. In the implementation the mean between the two channel responses is taken. h_0, h_1 denote the channel attenuation and its progression in time direction.

4.3 Space-Frequency transmission

Another possibility to implement the Alamouti scheme with OFDM is called Space-Frequency encoding. Here we place all Alamouti symbols within one OFDM symbol.

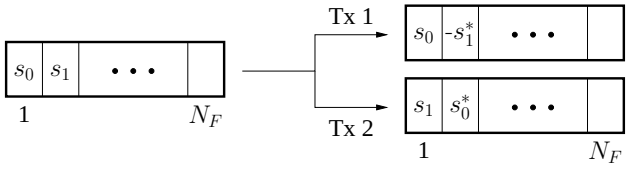

Figure 26: Principle of Alamouti Space-Frequency coding over OFDM

Figure 26 shows the principle of Space-Frequency Code (SFC). Here always neighbouring frequencies are used to get the constant component required by the Alamouti scheme. It is assumed that the channel does not change over two adjacent carriers. This assumption is hardly fulfilled for very frequency selective

channels. Besides it has problems with narrow-band distortion. Therefore we expect a loss of performance in this case. In figure 27 a frequency selective channel is illustrated to visualise the effect of a varying channel impulse responses of neighbouring frequencies.

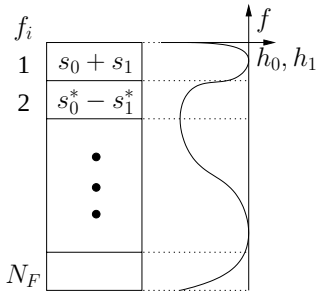

Figure 27: Problems of Space-Frequency coding over OFDM

After the modulation of the information bits to the modulation alphabet A_x blocks of N_F symbols are defined which equals to one OFDM symbol. Two adjacent symbols on position i respective $i+1$ with $0 \leq i \leq N_F - 1$, $i \mod 2 = 1$ form s_0 respective s_1. Therefore the number of carriers N_F has to be a multiple of 2. The sequence is then split up into two streams, one for each antenna. On Tx 1, position i we put s_0 and on $i+1$ the symbol $-s_1^*$ is set. For Tx 2 on the corresponding places s_1 and s_0^* are put.

In contrast to the Space-Time encoding principle we do not have a delay of one OFDM symbol with N_F samples.

4.4 Simulation results

In figure 28 the bit error rates for an uncoded OFDM transmission and Alamouti with Space-Time respective space-frequency encoding are compared. The channel is a one-path Rayleigh fading channel and OFDM with 64 carriers is used. For a velocity of $v = 0$ km/h we notice no difference between the two Alamouti implementations. Both types should work with best performance because all possible negative influences as e.g. velocity for Space-Time respective frequency selectivity for Space-Frequency transmission are excluded.

For low SNR values we can improve the BER with these diversity methods from 10^{-1} to $7 \cdot 10^{-2}$ but due to the higher slope of the Alamouti curves we can achieve an improvement of over two decades for higher SNRs. Using a convolutional

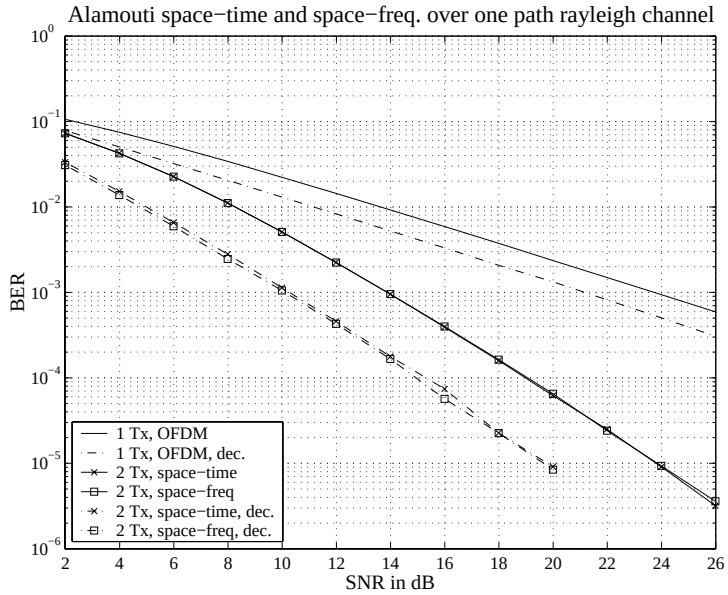

Figure 28: Comparison of Space-Time with Space-Frequency for $v = 0$ km/h over a Rayleigh channel

$(5,7)_{oct}$ code we can then ameliorate the BER in addition by about a decade or 4 dB and about 11dB at a BER of 10^{-3}.

Now we want to investigate the behaviour of the presented encoding schemes Space-Time and Space-Frequency. We have a look at their performance on time respective frequency variant channels. Besides we want to consider the influence of the assumption that the channel has to be constant during two consecutive symbols s_0 and $-{s_1}^*$ for Tx 1 respective s_1 and ${s_0}^*$ for Tx 2. Especially we are interested in the impact of the new channel matrix $\mathbf{C}$ from equation (33) which drops the premise made above.

First we look at Space-Frequency encoding and frequency selective channels. To increase the variance continuously we choose a two-path channel model with one tap at time $t_1 = 0$ and the second one at $t_2 > 0$ can be varied. Both paths have equal power. By increasing the delay t_2 of the second signal path we get additional variation in the spectrum. Therefore the difference between adjacent subcarriers extends more and more. Alamouti's assumption of equal channel values for consecutive symbols gets worse. At this point we want to compare the two implementations proposed in subsection 4.1. The new method does not require a constant channel for both symbols and therewith we expect to be less prone to the negative effects of a variant channel.

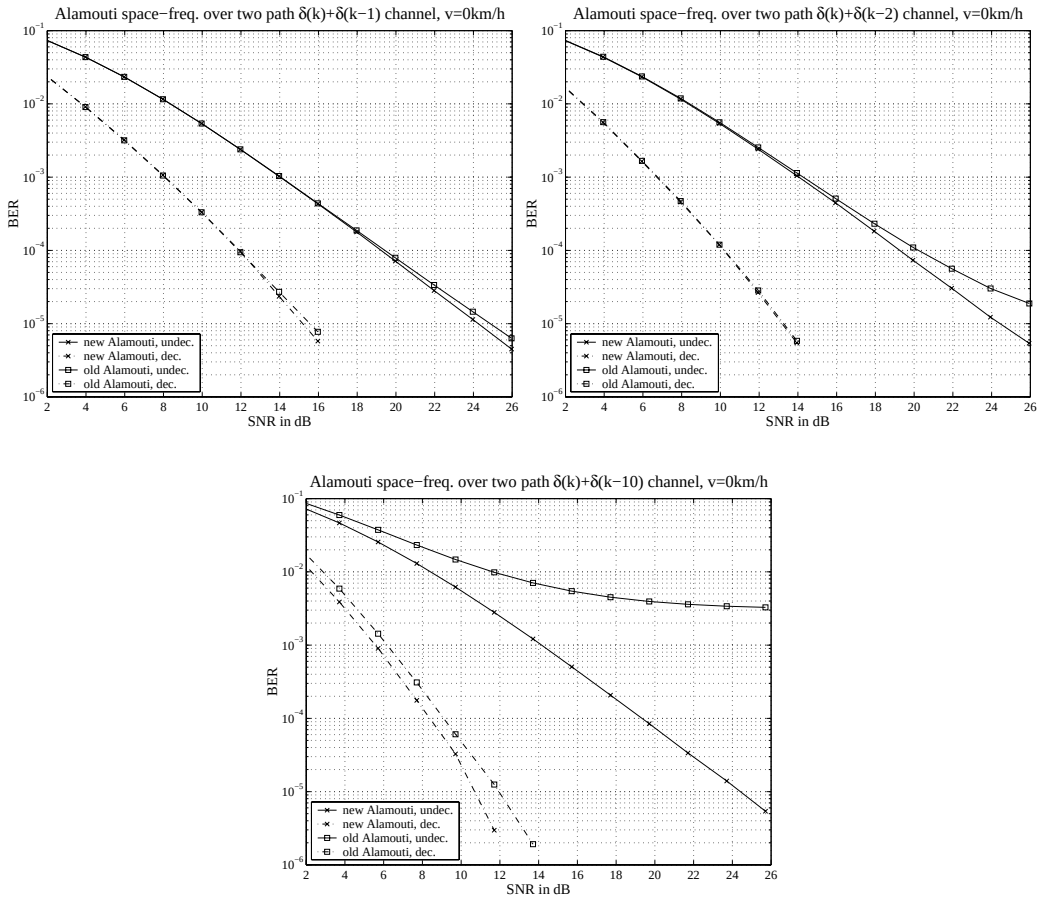

Figure 29: Comparison of the old and new Alamouti scheme for Space-Frequency encoding and different two tap channels

In figure 29 the BERs for three different two-path channels are plotted. The velocity of the mobile receiver is set to $v = 0$ km/h to exclude the influence of a temporal variation. We notice that with increasing frequency selectivity and higher SNR the undecoded BER curves diverge more and more. With the new method we reach approximately the results presented in figure 28. Whereas the original scheme suffers from the unmatched channel values. This becomes more and more visible for higher SNR values because the influence of the additive gaussian noise reduces and the problems due to the channel variation become the dominating effect. The BER then comes to an error floor. By using the new scheme we do not have these restrictions.

Using a convolutional $(5,7)_{oct}$ code we obtain less different results for the considered SNR range. Only for the $\delta(k) + \delta(k-10)$ channel they become visible. Due

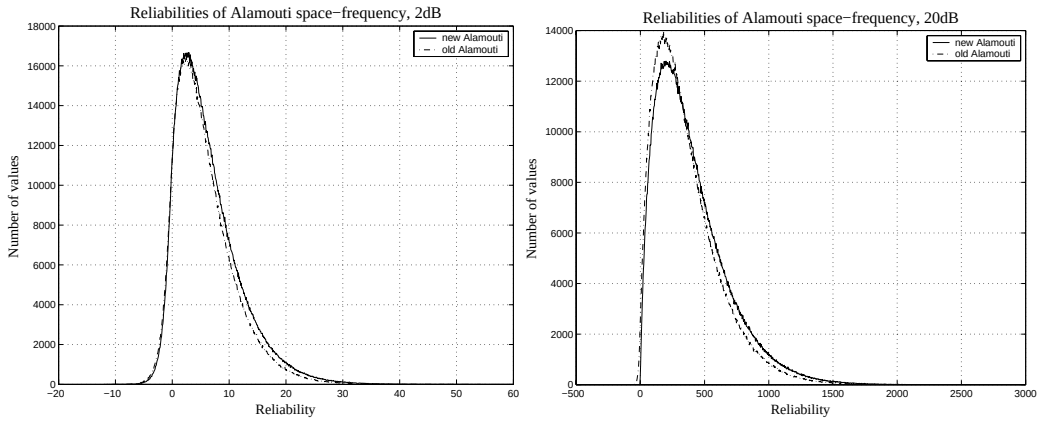

Figure 30: Comparison of the reliabilities for the two-path channel $\delta(k)+\delta(k-10)$, $v = 0$ km/h

to the occurrence of an error floor in the undecoded results we expect the same behaviour with channel coding. The problem is to sustain reliable simulation results for bit error rates (BER) where this effect appears. As a rule of thumb we need at least 100 bit errors to obtain stable results. For the appropriate SNRs we would approximately achieve a BER of 10^{-7}. This requires to simulate about 10^9 bits. In this thesis it cannot be evaluated in a reasonable time period.

The histograms in figure 30 point out the effects. We transmit our complex symbols and multiply the soft values of each bit from the Alamouti decoder with the BPSK modulated sent sequence (respective we map the source bits according to BPSK). Therefore we obtain a negative sign for an undecoded bit error. A high absolute value on the horizontal axis indicates a high reliability. For the left histogram (2dB) we notice the high number of undecoded errors resulting from the low SNR. Further the reliabilities for correct bits using the new channel matrix $\mathbf{C}$ are slightly higher. These two perceptions explain the differences in the decoded BER curve as well. For higher SNR both maxima move towards higher reliabilities. But the run of the curves diverge more and more. The original Alamouti scheme produces more undecoded bit errors which becomes visible in the higher number of values in the negative half-plane. Further we notice that the new Alamouti decoding scheme produces more trustworthy and therefore less uncertain values leading to a better decoding performance.

In the following we want to investigate the effects of the velocity on the behaviour of a Space-Time encoded Alamouti transmission. We also compare the two implementations with each other. From subsection 2.3 we already know that OFDM itself looses BER performance for higher velocities due to the Doppler shift and loss of the channel orthogonality.

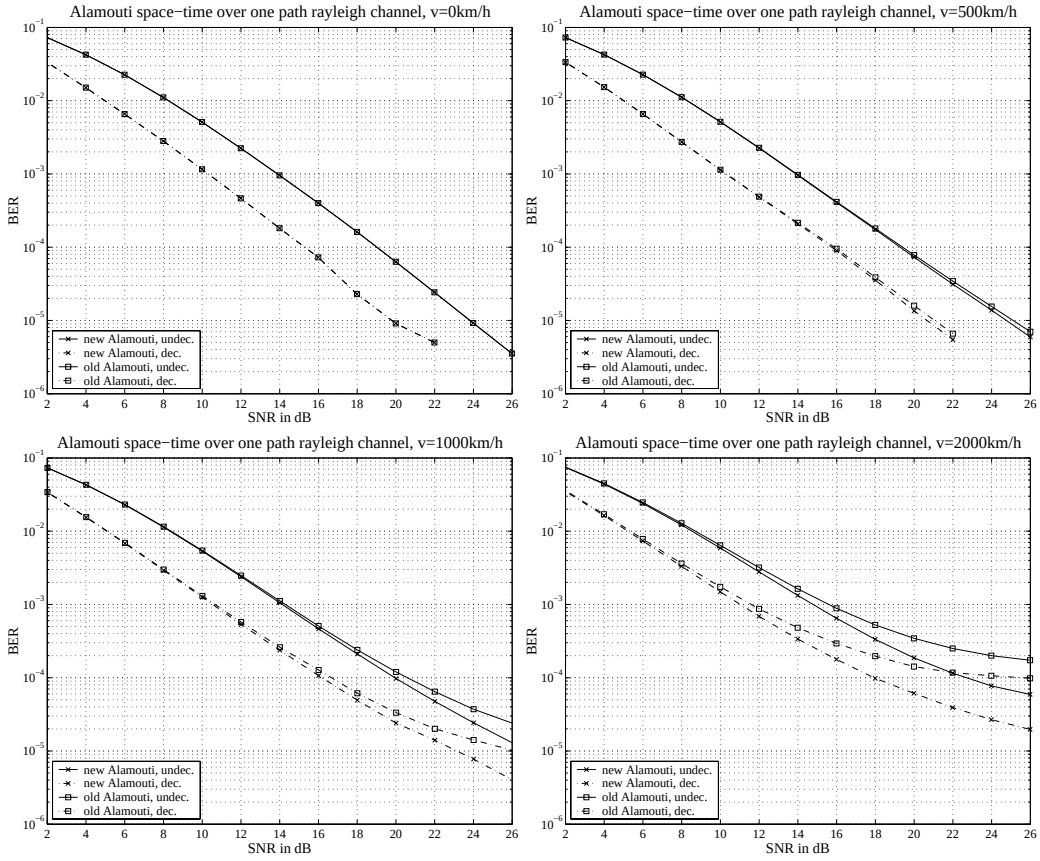

Figure 31: Comparison of the old and new Alamouti scheme for Space-Time encoding and different velocities

In figure 31 the BERs for four different velocities are plotted. As expected we do not notice any differences between the two implementation types for a standing receiver and there is no degradation. The corresponding channel values for each antenna are identical and therefore we cannot gain performance for this scenario. For increasing velocities both types show similar behaviour of the decoded and undecoded BER curves. This is mainly caused by the underlying OFDM. But the effect is more distinct for the original Alamouti scheme which suffers from the increasing discrepancy between consecutive channel values. For high speeds we even come to an error floor. At least we can lower this borderline with the new scheme.

Finally we want to compare the Space-Time and Space-Frequency encoding scheme (both in the new implementation form) for different velocities. In figure 32 the undecoded bit error rates for both types are plotted. Due to the usage of an one-path Rayleigh channel we face flat-fading. Therefore we do not get any

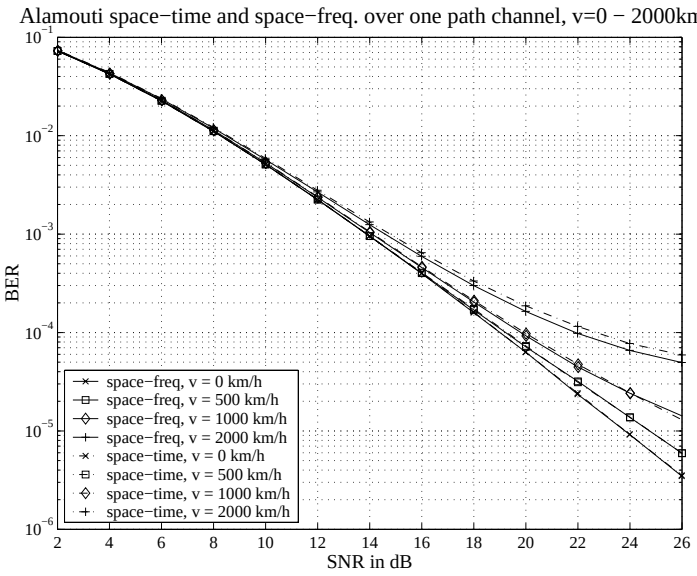

Figure 32: Comparison Space-Time with Space-Frequency for $v = 0 - 2000$ km/h over a one-path Rayleigh channel

influence of varying consecutive symbols using Space-Frequency encoding. For low velocities we obtain approximately the same bit error rates for both schemes. Only for very high speeds we notice small differences with benefits of the Space-Frequency scheme.

4.5 Conclusion

In this section we have investigated the Alamouti scheme and its implementation in OFDM. The combination provides two possibilities: Space-Time (STC) and Space-Frequency (SFC) encoding which differ in the manner of the symbol placing. Further a new method to overcome the premise of a constant channel over two consecutive symbols is presented. It only works for the description form presented in [18] but improves the encoding performance especially on varying channels. Therewith we are able to add a certain robustness against a changing channel to the transmission scheme.

5 Combination of Alamouti and CDD

In this section we want to investigate the combination of the Alamouti scheme with Space-Frequency Coding (SFC) and Cyclic Delay Diversity (CDD). But first we want to explain why this can be necessary.

For two antennas we already exploit full spatial diversity with Alamouti's scheme [20]. Further we do not have to assume a constant channel over two consecutive symbols anymore (confer to subsection 4). But we still face the problem of the extension to multiple transmit antennas. In [20] an orthogonal design for more than two antennas is proposed which is based on the Alamouti scheme. For real valued transmission and an arbitrary number of antennas we can thereby achieve maximum rate. But for complex valued signals we face the problem of a rate loss for more than two antennas.

We want to use another approach to extend the Alamouti scheme to more antennas which is presented in the following.

Considering equation (33) we have already noticed that we can treat each row in the matrix $\mathbf{C}$ (equals to consecutive time slots) independently. Therefore we can rewrite it to

$$\mathbf{C} = \begin{pmatrix} h_0 & h_3 \\ h_2^* & -h_1^* \end{pmatrix}. \tag{34}$$

Using two antennas which are far enough apart (approximately more than 10 wavelengths [1]) cause the two channels to be uncorrelated. Differing to the assumptions in the previous section we now assume that h_0 and h_1 respective h_2 and h_3 from equation (34) are uncorrelated, too. Then there is no reason to send the (negative) complex conjugated second symbol in the second time slot but just the second symbol. We get the same results (in average!) as long as we ensure full rank of $\mathbf{C}$. The problem is that we normally do not face a temporal or in frequency direction uncorrelated channel. But this would lead to a severe degradation of the system performance. From section 3 we know that CDD introduces virtual paths and causes additional frequency selectivity. Our approach is that adjacent carriers are pseudo-decorrelated to achieve similar bit error rates as an Alamouti encoded scheme for Rayleigh fading.

To get a measure for the correlation of consecutive channel values we have to use probability theory. The correlation coefficient $\rho_{X,Y}$ denotes the similarity of two random variables X and Y. It is defined as follows:

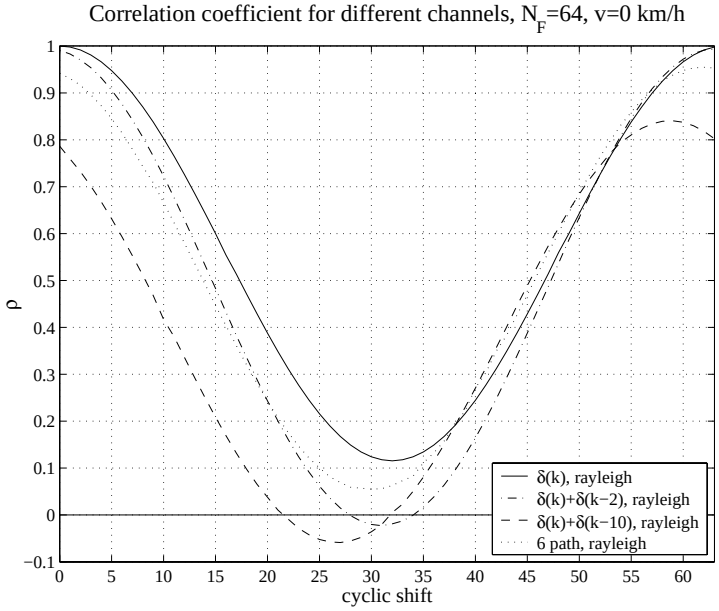

Figure 33: Correlation coefficients

$$\rho_{X,Y} = \rho(X,Y) = \frac{\mathrm{cov}(X,Y)}{\sqrt{\sigma_X^2 \sigma_Y^2}} = \frac{E\{(X-\mu_X)(Y-\mu_Y)\}}{\sigma_X \sigma_Y}. \tag{35}$$

In equation (35) $\mathrm{cov}(X,Y)$ denotes the covariance of X and Y and σ_X^2 respective σ_Y^2 are the variances. $E\{\cdot\}$ specifies the expectation and $\mu_X = E\{X\}$ respective $\mu_Y = E\{Y\}$ are the means. $\rho_{X,Y}$ fulfils following condition:

$$-1 \leq \rho_{X,Y} \leq 1. \tag{36}$$

A high absolute value of $\rho_{X,Y}$ denotes a high correlation whereas $\rho_{X,Y} = 0$ equals to uncorrelated variables X and Y [10].

In figure 33 the correlation coefficient is plotted in dependence on the cyclic shift and the type of channel. It is calculated assuming a Space-Frequency transmission and BPSK modulation. Therefore $\rho_{X,Y}$ is determined using adjacent carriers for the random processes X respective Y. They correspond to the transmit symbols s_0 and s_1 from the Alamouti scheme. As already mentioned above we are interested in decorrelation to get best results. For a fully correlated one-path channel with flat-fading characteristics and no cyclic shift we obtain the maximum correlation coefficient of 1. With an increasing shift to half of the carrier number we get more and more decorrelation up to 0.12. Further we notice the symmetry of

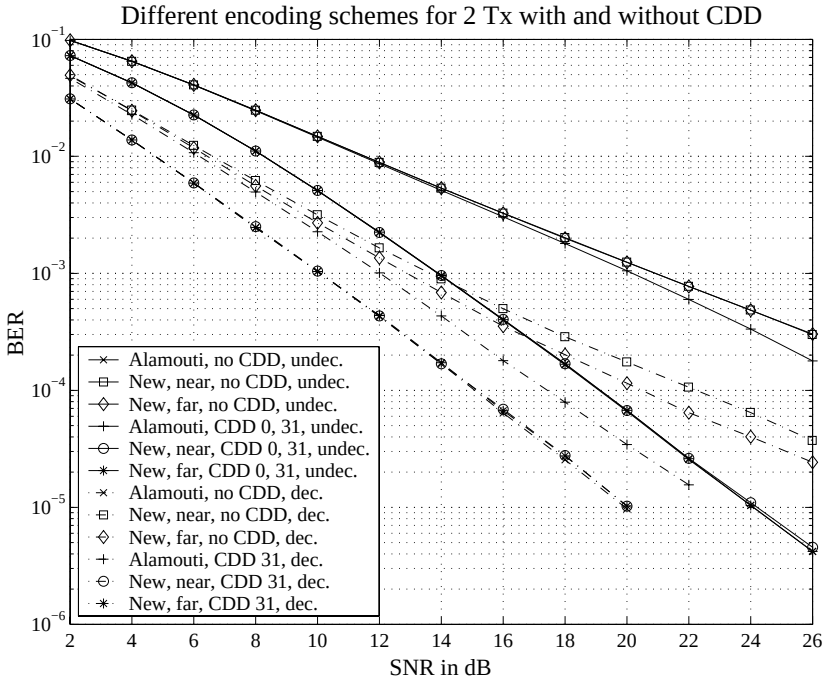

Figure 34: Bit error rates for different encoding schemes with and without cyclic shift over an one-path Rayleigh channel

the curve. For an already frequency selective channel the correlation can be lowered using CDD. Interesting is the comparison between the one- and the two-path channel $\delta(k)+\delta(k-10)$. The correlation coefficient curve of the two-path channel is cyclically shifted by 10 to the left and to approximately 0.16 down. Frequency selective channels show a basic decorrelation depending on their tap profile. But as a rule of thumb we can assume that a cyclic shift of 0 and $N_F/2$ leads to a sufficiently uncorrelated channel for two antennas. Further only BPSK modulation is considered. There might be different results for higher level modulation especially if they have a complex constellation.

Another possibility would be not to use adjacent carriers (near encoding), but to take most distant ones (far encoding). This can be done by utilising the carriers $1,\ldots,N_F/2$ for X and for Y the corresponding from the set $N_F/2+1,\ldots,N_F$. Then a minimum spacing of $N_F/2$ subbands can be achieved. The correlation coefficients for far encoding and different cyclic shifts is not plotted because we cannot improve the decorrelation result. Then $|\rho_{X,Y}|$ toggles between the minimal and maximal correlation coefficient of the results using neighbouring carriers. An even cyclic shift leads to a high value and an odd shift to a low value.

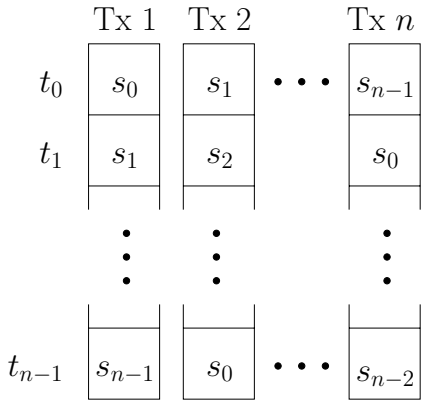

Figure 35: Encoding scheme for $n = N_{Tx}$ antennas

Now we have a look at the impact on the bit error rates of the described transmission methods. In figure 34 the BERs for Alamouti and the new scheme (near and far encoding) are plotted. The solid line corresponds to undecoded transmissions and the dash-dot curves to the appropriate decoded result. We notice that Alamouti with no CDD and both new schemes with CDD 31 lead to the same BER performance (decoded and undecoded). Combining cyclic shift and Alamouti causes severe degradations in the transmission characteristics. In other words the Alamouti scheme cannot be improved using CDD. It can only achieve similar results compared with the unshifted new schemes. Last mentioned are equal for the undecoded case which is reasonable because we use a flat-fading Rayleigh channel. The decoded results differ because the far encoding spreads the error patterns more and this leads to a lower error density. On the other hand the near scheme causes more adjacent erroneous undecoded bits which is less suited for the used convolutional $(5,7)_{oct}$ decoder.

The next step is the extension to more antennas. The scenario presented above is only the special case for two. For $N_{Tx} \geq 1$ antennas we need N_{Tx} symbols s_i with $i = 0, \ldots, N_{Tx} - 1$ to be transmitted. They are distributed on the antennas by performing a cyclic shift of one step as visualised in figure 35. Therefore we send in every time slot all symbols s_i. This enables us to extend the new scheme to an arbitrary number of transmit antennas N_{Tx}. A restricting drawback is an exponentially increasing decoding complexity

$$\text{decoding complexity} \sim M^{N_{Tx}}$$

where $M = |A_x|$ denotes the number of transmit symbols in the modulation alphabet A_x.

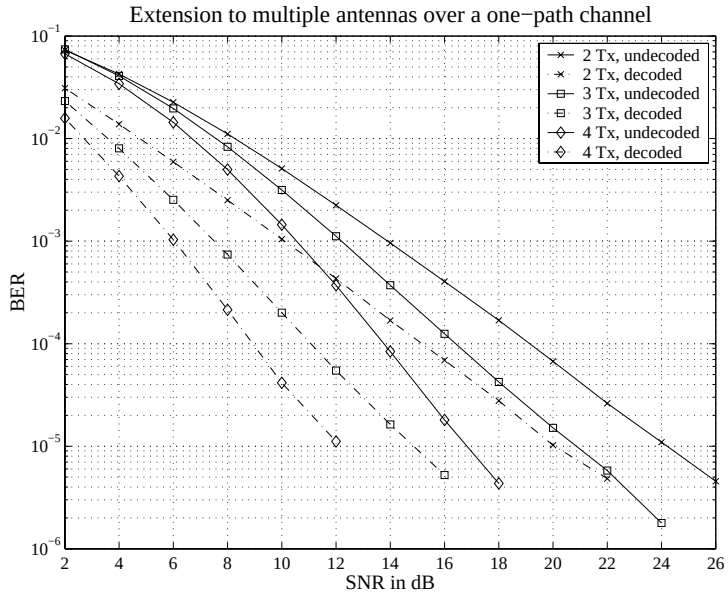

Figure 36: Bit error rates of two, three and four transmit antennas over an one-path Rayleigh channel

Now we investigate the results of the extension to multiple antennas. In figure 36 the BERs for two to four transmit antennas are depicted. We notice the diverging curves resulting from the different slopes. The gradient gets steeper with an increasing number of antennas. Therefore we get the desired improved performance in trade off with higher expenses. This means that we can weigh between a bit error rate gain on the one hand and extra efforts with regard to costs and decoding complexity on the other hand.

Comprising we can note that a combination of a scheme based on Alamouti and CDD can achieve same performance than pure Alamouti for two antennas and BPSK modulation. Further on it can easily be extended to an arbitrary number of antennas to obtain even better bit error rates. But then we have to accept the exponentially (with the number of antennas) rising decoding complexity. This leads to higher demands on the receiving device.

6 Conclusion

In this thesis two principle methods for spatial transmit diversity in combination with underlying OFDM are investigated.

In section 2 we first investigate and describe OFDM itself. The basic transmission model used in this work is presented and the two forms of realisation are explained. Further on we have a closer look at the channel and its transformation into several subchannels. Besides the sensitivity of higher velocities is investigated and properties of an OFDM transmission chain is discussed.

Section 3 deals with the topic delay diversity with special consideration of the cyclic form (CDD). It introduces virtual paths and increases the frequency selectivity. Therefore the undecoded error patterns are changed but the total number of errors remains constant. This enhances the decoder performance. The scheme is compared with interleaver with different window sizes. We can increase the number of antennas to further improve the decoded results.

In section 4 the Alamouti scheme is presented and discussed. It is extended to provide soft values and modified to be more resistant against fast varying channels. Together with OFDM there are two implementation possibilities namely Space-Time (STC) and Space-Frequency (SFC) encoding. They are used for the simulation to determine and explain the BER performance gains of the new scheme for different channel scenarios.

In the last section 5 a combination of CDD and a variation of the Alamouti scheme is discussed. Its main purpose is the simple extension of an Alamouti based spatial diversity scheme to an arbitrary number of antennas. Simulations for two antennas result in equal performance compared to the Alamouti scheme. Using more than two improves the BER performance further on and the slope increases, too.

A Appendix

A.1 List of variables

N	Number of antennas
N_F	Number of carriers
N_G	Length of guard interval in chips
N_{Tx}	Number of transmit antennas
$T_{s,\,0}$	Sampling time before OFDM modulation
T_s	Sampling time after OFDM due to upsampling for impulse shaping
$W = 1/T_s$	Bandwidth
$T_{symbol} = N_F \cdot T_s$	Usable OFDM symbol duration
$T_{guard} = N_G \cdot T_s$	Guard time duration
$T_{OFDM} = (N_F + N_G) \cdot T_s$	Total OFDM symbol duration with guard time
$f_{D,\,max}$	Maximum Doppler shift
f_c	Carrier frequency
τ_m	Maximum channel delay
A_x	Modulation alphabet
m	number of bits per symbol respective encoder memory
σ_n	Variance of noise
N_0	Noise power
Δf_c	Coherence bandwidth
ΔT_c	Coherence time
C_i	Channel capacity of the i-th carrier
C	Channel matrix
h, H	Channel values obtained from estimation H: DFT transformed
v	Velocity of mobile receiver
P_B	Bit error rate (BER)
δ_n	Time shift for Delay Diversity (DD)
$\delta_{cy,\,n}$	Cyclic time shift for Cyclic Delay Diversity (CDD)

A.2 List of abbreviations

AWGN	Additive White Gaussian Noise
BER	Bit Error Rate
BPSK	Bipolar Phase Shift Keying. Bit mapping: $0 \rightarrow 1$, $1 \rightarrow -1$
CDD	Cyclic Delay Diversity
DD	Delay Diversity
DFT	Discrete Fourier Transform
FFT	Fast Fourier Transform
ICI	Inter-Channel-Interference
IDFT	Inverse Discrete Fourier Transform
IOFDM	Inverse Orthogonal Frequency Division Multiplexing
ISI	Inter-Symbol-Interference
MMSE	Minimum Mean Square Errors (equalisation)
OFD	Optimum Free Distance (of convolutional codes)
OFDM	Orthogonal Frequency Division Multiplexing
PD	Phase Diversity
PDF	Probability Density Function
Rx	Receive antenna(s)
SFC	Space-Frequency Code
SNR	Signal-To-Noise Ratio with noise power N_0 and variance $\sigma_n^2 = N_0/2$
STC	Space-Time Code
Tx	Transmit antenna(s)
WSSUS	Wide Sense Stationary Uncorrelated Scattering (channel model)
ZF	Zero-Forcing (equalisation)

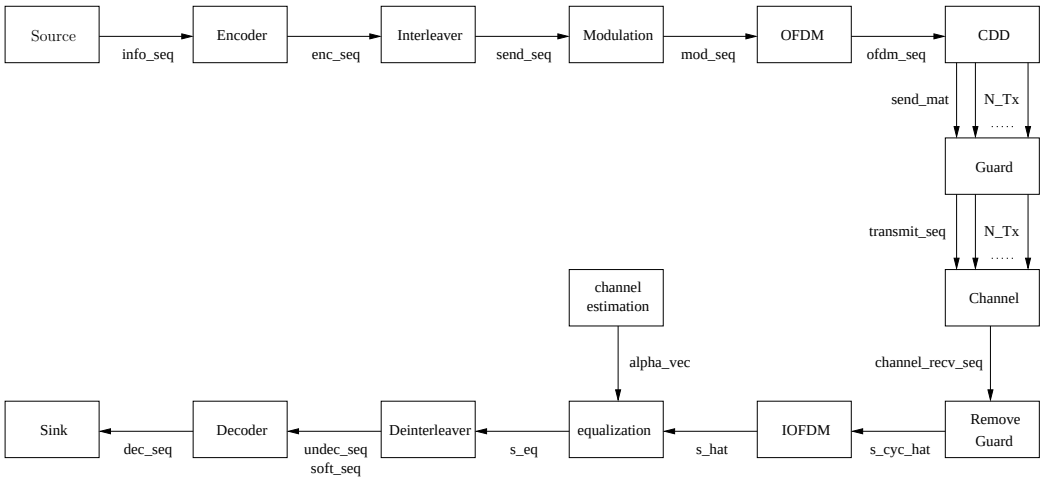

Figure 37: Block diagram of the whole CDD transmission

A.3 Implementation issues of the CDD simulation

In figure 37 the block diagram of the CDD over OFDM transmission with the variable names used in the source code is given. For reproducibility and compatibility reasons all "random"[1] processes (information sequence, AWGN, channel, and random interleaver) have their own seed. Each SNR value therefore has the same information sequence, interleaver performance and channel behaviour. As transmission parameters we have a carrier frequency of $f_c = 5150$ MHz and a bandwidth of $W = 1/T_{s,0} = 100$ MHz (no upsampling). Further on a terminated OFD convolutional code $(5,7)_{oct}$ with rate $1/2$ is used. The encoded sequence is then modulated using BPSK alphabet. Before the transmission it is normalised with $\sqrt{N_{Tx}}$ to achieve same power level for different number of transmit antennas.

The channel is simulated using a WSSUS (wide sense stationary uncorrelated scattering) channel model with parameters specified e.g. in table 1 and afterwards white gaussian noise is added to simulate the noise coming from the reception electronic assembly. Besides the σ_n of the complex AWGN is (according to the international definition) calculated as follows:

$$\sigma_n = \sqrt{\frac{N_0}{2}} = \sqrt{\frac{10^{\frac{SP|_{dB} - SNR|_{dB}}{10}}}{2}}$$

with noise power N_0 and $SP|_{dB} = 0$ dB which equals to a signal power of 1 because the transmit sequence is normalised to this value. $SNR|_{dB}$ is the given Signal-to-

[1] In fact it is only a pseudo-random process with a seed to reproduce the numerical order

Noise Ratio. Due to the Raleigh fading characteristics of the channel model the correct SNR value has to be shifted according to

$$SNR_{real}|_{dB} = SNR_0|_{dB} + P_{recv}|_{dB} - P_{send}|_{dB}$$

where $SNR_0|_{dB}$ is the desired value and $P_{recv}|_{dB}$ and $P_{send}|_{dB}$ are the receive respective send powers of the sequences. No further normalisations (e.g. due to the guard time) are performed. Furthermore a channel estimation is performed by simulating the impulse response of the respective channel without the additive white gaussian noise. This leads to a perfect estimation for $v = 0$ km/h but for higher velocities the influence of the changing channel during the symbol becomes more visible. Therefore the quality of the estimation gets worse. The channel entree is changed in predefined intervals to simulate different “scenarios”. Using this feature a perfect channel estimation can be implemented by setting the velocity to zero and reinitialising the channel after every symbol. Normally a speed of $v = 200$ km/h and a change process of 15 OFDM symbols (including the guard time) are set.

On the receiver side a Zero-Forcing equalisation is performed after the IOFDM using the DFT transformed of the channel estimation normalised by $\sqrt{N_F}$. Further on critical positions (from the numerical point of view) are eliminated which means that channel values less than ε are set to 1. For soft decision Viterbi decoding the received and equalised sequence has to be multiplied with the absolute square of the Zero Forcing values to even the introduced SNR fluctuations.

- also see section power requirements, delay effects and antenna configuration

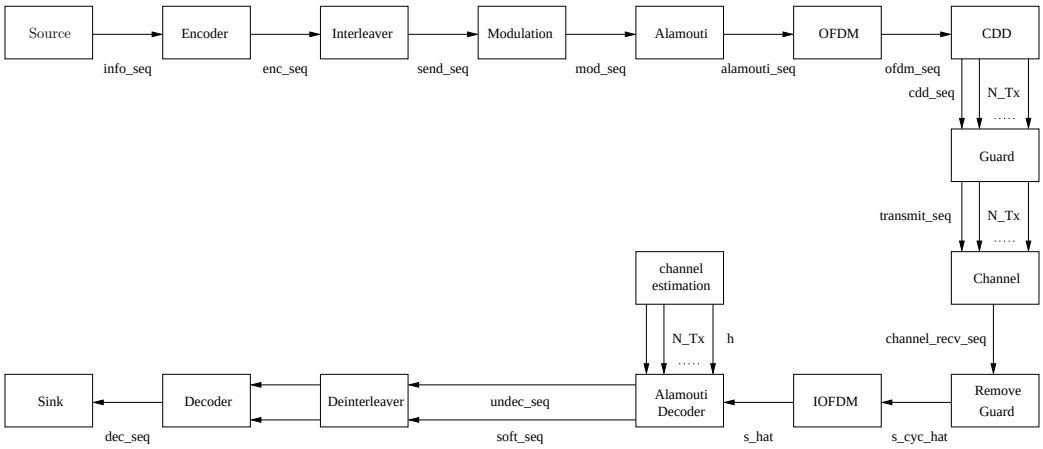

Figure 38: Block diagram of the whole Alamouti transmission

A.4 Implementation issues of the Alamouti simulation

Figure 38 depicts the block diagram of the whole Alamouti transmission used in this thesis. Basically it is similar to the one used for CDD with some exception and supplements. Therefore we only want to consider the differences.

As far as the Alamouti encoder we do not make any distinctions. Then we perform an Alamouti encoding according to the desired scheme. We can choose between Space-Time, Space-Frequency and our new scheme. Last mentioned can use more than two antennas. Afterwards an OFDM encoding for each antenna and the appropriate cyclic shifts are performed. Finally the guard interval is added. Then the sequence is transmitted.

For each antenna a channel estimation has to be performed. Thereby we have to consider the corresponding cyclic shift. In the simulation the estimation is done using a Dirac impulse which is positioned directly after the guard interval. Additionally we have to shift it according to the specific antenna shift. As channel we use the already described WSSUS model. As explained in the CDD appendix we randomly change the channel state every OFDM symbol respective every second symbol for Alamouti Space-Time encoding. As carrier frequency $f_c = 5150$ MHz is used and the bandwidth is $W = 1/T_s = 20$ MHz.

On the receiver side we first perform an IOFDM and feed the result together with the channel and SNR estimations to the Alamouti decoder. It returns soft and hard decision results which are then deinterleaved and Viterbi decoded. The absolute of the soft values have a fixed upper limit to avoid numerical problems with the following decoding processes.

List of Figures

References

[1] S. M. Alamouti; *A simple transmit diversity technique for wireless communications*; IEEE journal on select areas in communications, vol. 16 no. 8; October 1998.

[2] J. Lindner; *Lecture "Advanced wireless multiuser communications"*; Department of information technology, University of Ulm; June 2000.

[3] M. Bossert; *Kanalcodierung*; Teubner, Stuttgart; 1998.

[4] R. W. Chang, R. A. Gibby; *A theoretical study of performance of an orthogonal multiplexing data transmission scheme*; IEEE transactions on communications technology vol. COM-16 no. 4, pp. 529-540; August 1968.

[5] Armin Dammann, Stefan Kaiser; *Low complex standard conformable antenna diversity techniques for OFDM systems and its application to the DVB-T system*; 2001.

[6] Adrian Donder; *Beiträge zur OFDM-Übertragung im Mobilfunk*; Ph.D. thesis, University of Ulm, Germany; 1999.

[7] S. Höst; *On woven convolutional codes*; Ph.D. thesis, Lund University, Sweden, September 1999.

[8] S. Höst, R. Johannesson, K. S. Zigangirov, V. V. Zyablov; *Active Distances for Convolutional Codes*; IEEE transactions on information theory, vol. IT-45, pp. 658-669; March 1999.

[9] R. Johannesson, K. S. Zigangirov; *Fundamentals of convolutional coding*; IEEE press, ISBN 0-7803-3483-3; 1999.

[10] F. Jondral, A. Wiesler; *Grundlagen der Wahrscheinlichkeitsrechnung und stochastischer Prozesse für Ingenieure*; Teubner Studienbücher Elektrotechnik; 2000.

[11] Stefan Kaiser; *Spatial transmit diversity techniques for broadband OFDM systems*; In proceedings IEEE global telecommunications conference (GLOBECOM 2000), pp. 1824-1828; November 2000.

[12] K. D. Kammeyer, U. Tuisel; *Synchronisationsprobleme in digitalen Multiträgersystemen*; FREQUENZ 47 5-6, pp. 159-166; 1993.

[13] J. G. Proakis; *Digital Communications*; Third edition, McGraw-Hill Book Co.; 1995.

[14] A. Ruiz, J. M. Cioffi, S. Kasturia; *Discrete multiple tone modulation with coset coding for the spectrally shaped channel*; IEEE transactions on communications technology vol. 40 no. 6, pp. 1012-1029; June 1992.

[15] H. Sari, G. Karam, I. Jeanclaude; *An analysis of Orthogonal Frequency Division Multiplexing for mobile radio applications*; In proceedings VTC'94, pp.1635-1639; 1994.

[16] B. R. Saltzberg; *Performance of an efficient parallel data transmission*; IEEE transactions on communications technology vol. COM-15 no. 6, pp.805-811; December 1967.

[17] W. Schnug, M. Bossert; *Iterative APP-Decodierung von Faltungscodes mit Hilfe von Prüfgleichungen*; Forschungsbericht DFG Projekt Bo 867/4-1, University of Ulm, department of information technology; April 1998.

[18] H. Schulze; *Simple transmit diversity for a convolutionally coded multicarrier QAM system*; 6th international OFDM workshop (InOWo), Hamburg; 2001.

[19] C. Sgraja; *Kombinierte Entzerrung und Decodierung bei Paketübertragungsverfahren mit allgemeinen komplexwertigen Modulationsverfahren*; Diploma thesis, department of information technology, University of Ulm; December 1998.

[20] V. Tarokh, H. Jafarkhani, A. R. Calderbank; *Space-time block codes from orthogonal designs*; IEEE transactions on information theory, vol. 45, pp. 1456-1467; July 1999.

[21] S. B. Weinstein, P. M. Ebert; *Data transmission by frequency-division multiplexing using the discrete fourier transform*; IEEE transactions on communications technology vol. COM-19 no. 5, pp.628-634; October 1971.

[22] W. Y. Zou, Y. Wu; *COFDM: An Overview*; IEEE transactions on broadcasting vol. 41 no. 1, pp. 1-81; March 1995.